

CHAPTER 8

WHY PRECISELY SEVENTEEN TYPES?

8.0 Classification of wallpaper patterns

8.0.1 The goal. Back in section 2.8 it was rather easy to explain why there exist precisely **seven** types of **border** patterns. But we have not so far attempted to similarly **determine** the number of possible wallpaper patterns: we simply **assumed** that there exist precisely **seventeen** types of **wallpaper** patterns in order to investigate their two-colorings in chapter 6. And there was a good reason for this: unlike border patterns, wallpaper patterns may only be **classified** with considerable effort; in fact most known proofs would probably be too **advanced** mathematically for many readers of this book. Luckily, we are at long last in a position to fulfill our promise at the end of 4.0.6 and **justify** our assumptions on wallpaper patterns, classifying them in a purely **geometrical** manner: no tools beyond those already developed in earlier chapters will be needed.

Of course ‘half’ of our goal has already been achieved: chapter 4 provides some rather convincing evidence on the **existence** and **structure** of the seventeen types, and the latter has also been indirectly examined in chapters 6 and, to some extent, 7. What we need to reach now is a **negative** result: there cannot be any more types of wallpaper patterns other than the ones studied in chapter 4.

8.0.2 The tactics. The promised classification will be greatly facilitated by the **Crystallographic Restriction** of section 4.0, established in 4.0.6: the smallest rotation angle of a wallpaper pattern may only be 360^0 (none), 180^0 , 120^0 , 90^0 , or 60^0 . This fundamental fact allows us to **split** the entire classification process into **five** cases. Moreover, we will view each 90^0 pattern as

'built' on two 180^0 patterns, each of which will in turn be viewed as a '**product**' of two 360^0 patterns; and something quite similar will happen among 360^0 , 120^0 , and 60^0 patterns. This approach allows us to reduce potentially 'complicated' types to **simpler** ones.

As stated above, we will be looking for 'negative' results, trying to **rule out** various geometrical situations and, to be more specific, interactions among isometries. Therefore various facts on **compositions of isometries** explored in chapter 7 are going to be crucial. Moreover, looking at an isometry's **image** under another isometry will often be useful: that operation is closely related to the **Conjugacy Principle** of 6.4.4 (and 4.0.4 & 4.0.5), and needs to be further investigated before the classification begins.

8.0.3 The Conjugacy Principle revisited. First formulated in 6.4.4, the Conjugacy Principle essentially states that, given two isometries I and I_1 , I_1 's image under I , denoted by $I[I_1]$, is still an isometry, equal in fact to $I \circ I_1 \circ I^{-1}$ (and **not** $I \circ I_1$). In 6.4.4, figure 6.36, I was the glide reflection **G**, I_1 was the reflection **M**₁, and $I[I_1]$ was the glide reflection **M**₂. In 4.0.4, figure 4.4, I was the translation **T**, I_1 was the clockwise rotation **R** = (K, ϕ), and $I[I_1]$ was the clockwise rotation (**T**(K), ϕ). And in 4.0.5, figure 4.6, I was the clockwise rotation **R**₁ = (K₁, ϕ_1), I_1 was the clockwise rotation **R**₂ = (K₂, ϕ_2), and $I[I_1]$ was the clockwise rotation (**R**₁(K₂), ϕ).

One should be careful about what exactly $I[I_1]$ stands for! The following example, where I is the glide reflection **G** and I_1 is the **counterclockwise** rotation **R** = (K, ϕ) is rather illuminating:

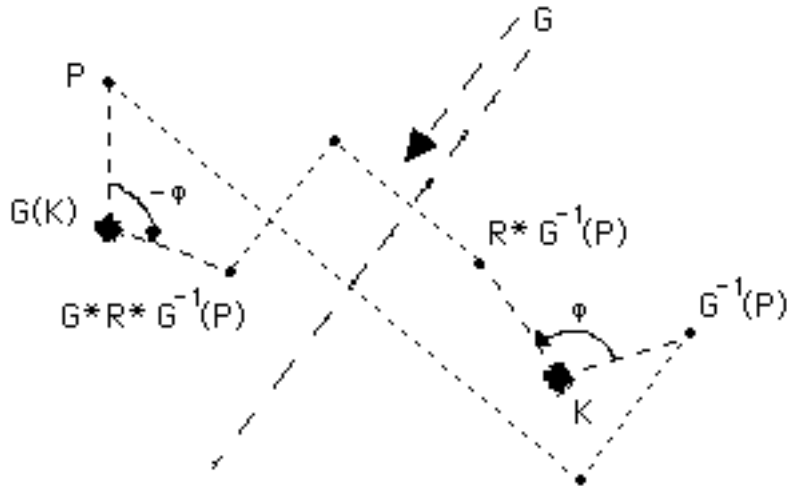


Fig. 8.1

As made clear by figure 8.1, $I[I_1] = I * I_1 * I^{-1}$ is the **clockwise** rotation $(\mathbf{G}(K), -\phi)$: \mathbf{G} glide-reflected not only \mathbf{R} 's center, but also the **arrow** indicating its orientation! This **empirical** 'arrow rule' works rather well: for example, it indicates -- by placing the arrows and the angles in a circular context, if needed -- that **rotating** a rotation I_1 by another rotation I should **preserve** its orientation, regardless of whether I is clockwise or counterclockwise; you should be able to verify this claim by considering all possible combinations of clockwise and counterclockwise in figure 4.6.

So far we have not said anything about **proving** the various instances of the Conjugacy Principle. Well, **congruent triangles** simply give everything away in figure 4.6, while the presence of **three parallelograms** settles everything in figure 4.4. And in figure 8.1 above, where we are facing a seemingly more difficult situation, a seemingly cleverer but merely **generalizing** approach works: the triangle $\{P, \mathbf{G}(K), \mathbf{G} * \mathbf{R} * \mathbf{G}^{-1}(P)\}$ is the **image** of the **isosceles** triangle $\{\mathbf{G}^{-1}(P), K, \mathbf{R} * \mathbf{G}^{-1}(P)\}$ under \mathbf{G} , therefore **congruent** to it; it follows that $\mathbf{G} * \mathbf{R} * \mathbf{G}^{-1}(P) = I * I_1 * I^{-1}(P)$ is indeed the image of P under the **clockwise** rotation $(\mathbf{G}(K), -\phi) = I[I_1]$, hence we may conclude that $I[I_1] = I * I_1 * I^{-1}$ holds.

The method employed in figure 8.1 could also be employed back in figures 4.4 & 4.6: it requires no particular skill or ingenuity, just

experience in arguing somewhat **abstractly**. But in figure 8.2 below -- an '**inverse**' of figure 8.1, for now we rotate a glide reflection instead of glide-reflecting a rotation -- there **seems** to be a complication: while K , P , and $R * G * R^{-1}(P)$ are clearly the images under R of K , $R^{-1}(P)$, and $G * R^{-1}(P)$, respectively, it is **not** obvious that P 's image under the rotated reflection line $R[M]$ is the same as $M * R^{-1}(P)$'s image under R ; notice that we do need this fact in order to show that the segment $\{R[M](P), R * G * R^{-1}(P)\}$ is **both** equal in length to the segment $\{M * R^{-1}(P), G * R^{-1}(P)\}$ and parallel to $R[M]$, therefore equal to the vector $R[T]$, as figure 8.2 suggests. (Recall at this point that isometries, and rotations in particular, map parallel lines to parallel lines (1.0.9).)

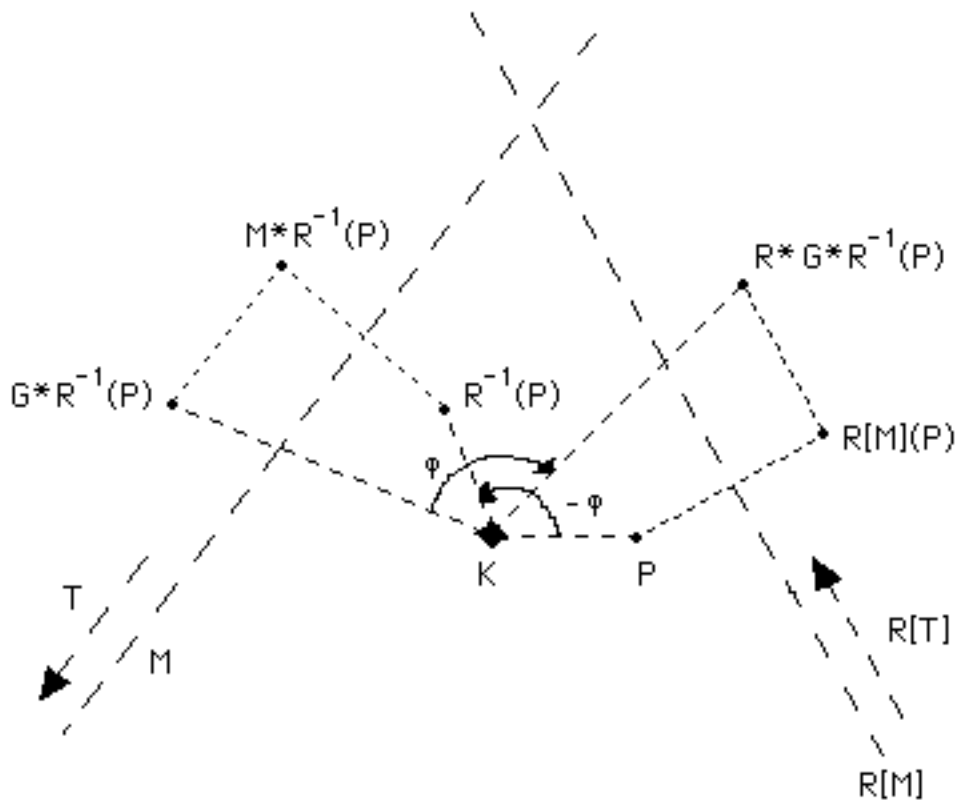


Fig. 8.2

So, how do we establish $R(M * R^{-1}(P)) = R[M](P)$? While a 'standard' geometrical approach is possible, the following idea, extending the methods of this section and suggested by **Phil Tracy**, is much more efficient: simply **rotate** the axis M along with the quadrangle $\{K, R^{-1}(P), M * R^{-1}(P), G * M * R^{-1}(P)\}$ to $R[M]$ and the

congruent quadrangle $\{K, P, R(M * R^{-1}(P)), R * G * R^{-1}(P)\}$; the desired equality $R(M * R^{-1}(P)) = R[M](P)$ follows now from the observation that isometries preserve perpendicular bisectors -- in particular R rotates the perpendicular bisector M of $\{R^{-1}(P), M * R^{-1}(P)\}$ to the perpendicular bisector $R[M]$ of $\{P, R(M * R^{-1}(P))\}$, so that $R(M * R^{-1}(P))$ is indeed the mirror image of P about $R[M]$.

We have just derived the most difficult case of the Conjugacy Principle, showing that the rotation of a glide reflection by an angle ϕ is another glide reflection **both** the axis and the vector of which have been rotated by ϕ : this will be useful in what follows, and so will be its 'inverse' on glide-reflected rotations (figure 8.1).

Here is a challenge for you concerning the image of a glide reflection under **another** glide reflection **not parallel** to it (a case that, unlike the previous ones, we do not need in the rest of this chapter): how would you 'justify' figure 8.3?

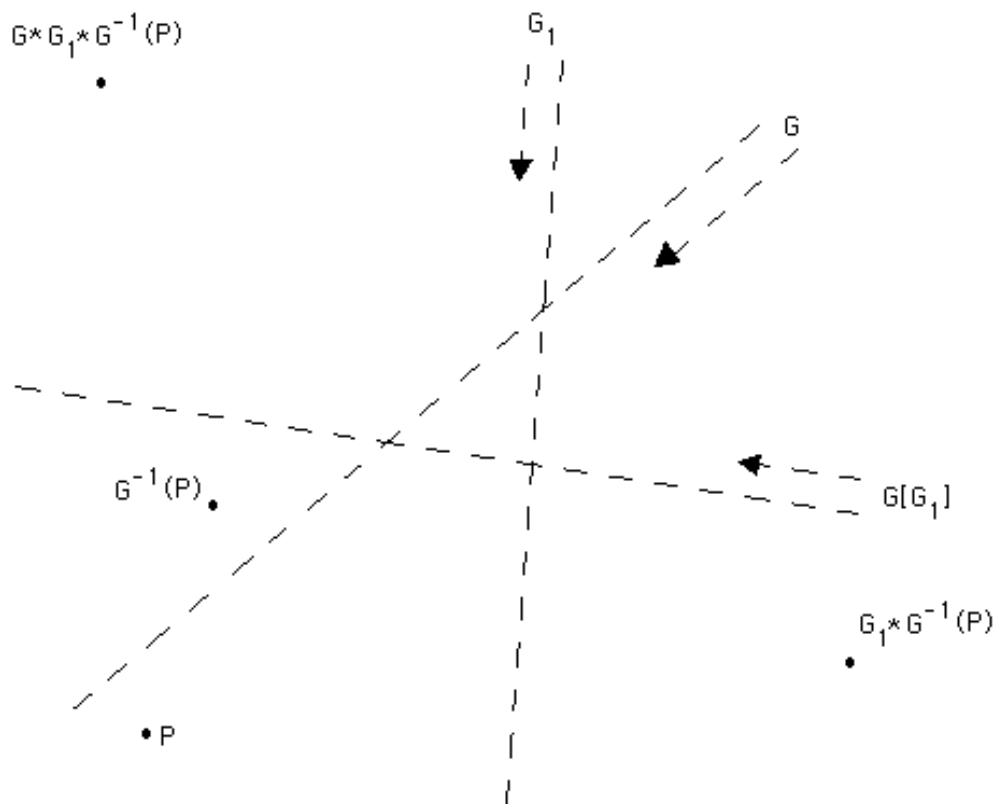


Fig. 8.3

Here is another useful instance of the Conjugacy Principle:

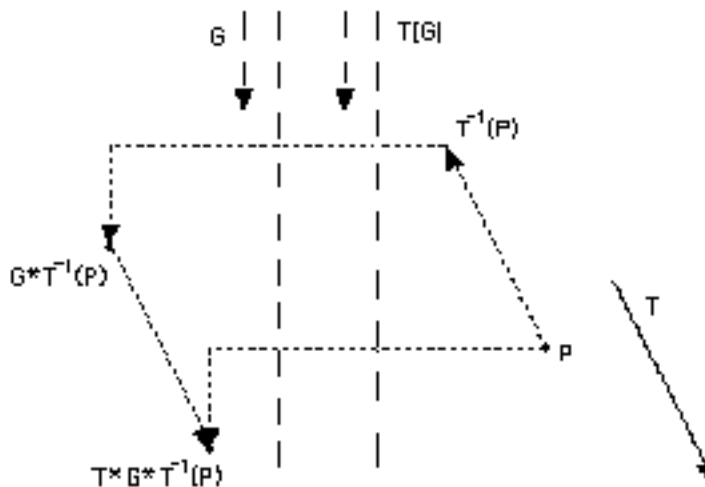


Fig. 8.4

A seasoned conjugacist by now, you should have no trouble understanding what happened in figure 8.4: you better do, it is destined to play a crucial role in what follows! (The few remaining cases and possibilities of the Conjugacy Principle are rather easier, and left to you to investigate; from here on we will assume it **proven** in full rigor and generality, but we will be explicitly stating where and how we use it throughout our classification of wallpaper patterns (sections 8.1-8.4).)

8.1 360° patterns

8.1.1 The basic question. The first question we will be asking in each of the coming sections is: does the pattern in question have (glide) reflection? In the case of a 360° pattern, a negative answer to this question implies a pattern that has **only** translation(s): that's our familiar **p1** pattern, and there is not much more to say about it than what we already discussed in sections 4.1 and 6.1.

8.1.2 How many (glide) reflections? An affirmative answer to the ‘basic question’ of 8.1.1 naturally raises the question: “how many kinds of (glide) reflection may coexist in a 360° pattern?” What we can say at once is that there **cannot** possibly be (glide) reflection in **two** distinct directions; indeed that is ruled out by the basic result of section 7.10 (which generalizes sections 7.2 and 7.9): any two (glide) reflections intersecting at an angle $\phi/2$ produce a **rotation** by an angle ϕ (7.10.2).

At the same time, the Conjugacy Principle yields infinitely many (glide) reflections derived out of the one that we started with. Indeed every wallpaper pattern has translation in **at least two** directions, in particular in a direction **distinct** from that of the given (glide) reflection; that translation T , as well as its **inverse** T^{-1} , simply translate the given (glide) reflection G -- as suggested in figure 8.4 -- again and again in both directions, creating an **infinitude** of **parallel** (glide) reflections of **equal gliding vectors**: $T[G]$, $T^2[G] = T[T[G]]$, ... , $T^n[G] = T[T^{n-1}[G]]$, ... and $T^{-1}[G]$, $T^{-2}[G] = T^{-1}[T^{-1}[G]]$, ... , $T^{-n}[G] = T^{-1}[T^{-n+1}[G]]$, ... (figure 8.5):

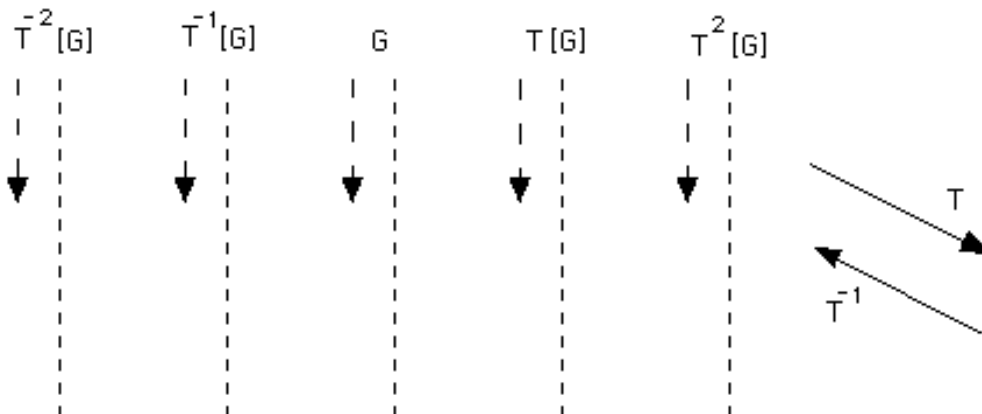


Fig. 8.5

8.1.3 Another way to go. Let's now employ composition of isometries (section 7.4) instead of the Conjugacy Principle, forming $T*G$, $T^2*G = T*(T*G)$, ... , $T^n*G = T*(T^{n-1}*G)$, ... and $T^{-1}*G$, $T^{-2}*G = T^{-1}*(T^{-1}*G)$, $T^{-3}*G = T^{-1}*(T^{-2}*G)$, ... , $T^{-n}*G = T^{-1}*(T^{-n+1}*G)$, ... :

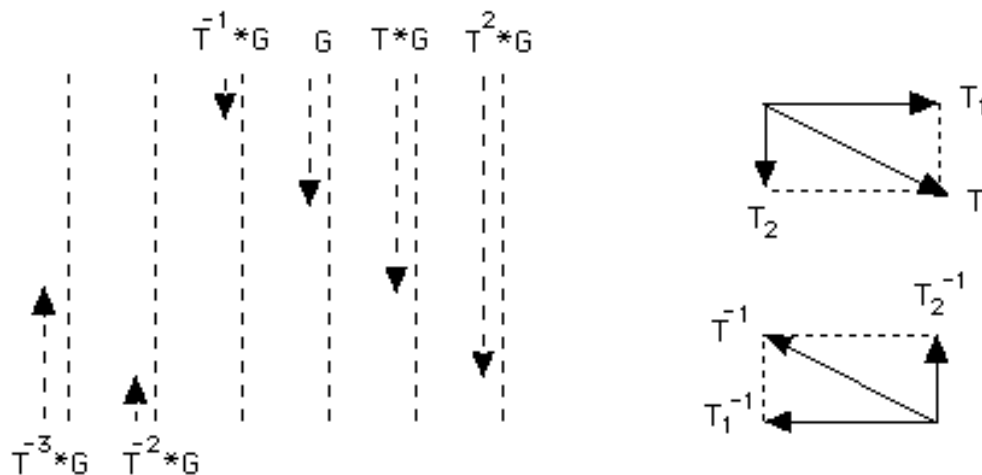


Fig. 8.6

Figure 8.6 certainly **looks** more complicated than figure 8.5, but it isn't; indeed it **essentially** consists, just like figure 8.5, of a **single** glide reflection, $\mathbf{G}_0 = \mathbf{T}^{-1} * \mathbf{G}$, with all others being **translated odd powers** of it: $\mathbf{G} = (\mathbf{T}_1/2)[\mathbf{G}_0^3]$, $\mathbf{T} * \mathbf{G} = \mathbf{T}_1[\mathbf{G}_0^5]$, $\mathbf{T}^2 * \mathbf{G} = (3\mathbf{T}_1/2)[\mathbf{G}_0^7]$, ... and $\mathbf{T}^{-2} * \mathbf{G} = (\mathbf{T}_1^{-1}/2)[\mathbf{G}_0^{-1}] = (-\mathbf{T}_1/2)[\mathbf{G}_0^{-1}]$, $\mathbf{T}^{-3} * \mathbf{G} = \mathbf{T}_1^{-1}[\mathbf{G}_0^{-3}] = (-\mathbf{T}_1)[(\mathbf{G}_0^{-1})^3]$, ... , where \mathbf{T}_1 and $\mathbf{T}_1^{-1} = -\mathbf{T}_1$ are \mathbf{T} 's and \mathbf{T}^{-1} 's perpendicular-to- \mathbf{G} components, respectively (figure 8.6). (In general, $\mathbf{T}^m * \mathbf{G} = ((\frac{m+1}{2})\mathbf{T}_1)[\mathbf{G}_0^{2m+3}]$, for **all** integers m ; of course this equation is valid **only** for the **particular** \mathbf{G} and \mathbf{T} in figure 8.6!)

What we used above is the fact that every pattern having glide reflection based on axis \mathbf{M} and **minimal** gliding vector \mathbf{T} is bound to **also** have glide reflections $(\mathbf{M}, k\mathbf{T})$, where k is an **odd** integer (positive or negative); **no** even multiples of \mathbf{T} are there because, as we saw as far back as 5.4.1 and 2.4.2 (**p1a1** border patterns), the **square** (and therefore every **even power**) of a glide reflection is a **translation** by a vector twice as long as the glide reflection vector. Conversely, every 'non-minimal' glide reflection combined with \mathbf{T} and its powers brings us back to the minimal one, (\mathbf{M}, \mathbf{T}) : in the context of figure 8.6, $\mathbf{G}_0^{2m+3} = \mathbf{T}^{m+1} * \mathbf{G}_0$ for **all** integers m .

One last remark before we go on: the compositions $\mathbf{G} * \mathbf{T}^m$ would

not bring any additional glide reflections into figure 8.6. You may verify that using again the techniques of section 7.4; in algebraic terms, notice some curious identities such as $\mathbf{G}*\mathbf{T} = (\mathbf{T}^{-1}*\mathbf{G})^3!$

8.1.4 Can they coexist? In view of our remarks in 8.1.2 and 8.1.3, figures 8.5 and 8.6 may be merged into one as follows:

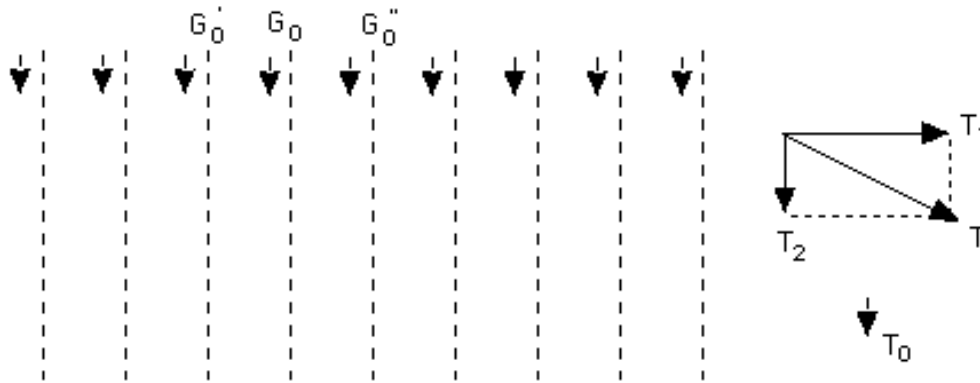


Fig. 8.7

In other words, we simply represent each one of infinitely many, parallel to each other glide reflections by its axis and **minimal** downward gliding vector \mathbf{T}_0 , remembering that all **odd multiples** of \mathbf{T}_0 (positive/downward or negative/upward) produce valid glide reflections based on the same axis. And what we obtained after all these deliberations is the rather familiar symmetry plan of a **pg** pattern! (Note at this point that \mathbf{T} 's components, $\mathbf{T}_2 = \mathbf{G}_0^2 = 2 \times \mathbf{T}_0$ and $\mathbf{T}_1 = \mathbf{G}_0 * \mathbf{G}'_0 = \mathbf{G}''_0 * \mathbf{G}_0$, are valid translations of this **pg** pattern, too.)

It seems that there is no problem at all here, but ... there is a catch! Indeed each glide reflection in figure 8.7 is a translate (**copy**) of $\mathbf{G}_0 = \mathbf{T}^{-1} * \mathbf{G}$ obtained in 8.1.3, but ... that's **not** the glide reflection \mathbf{G} that we started with in 8.1.2! To wit: had we assumed \mathbf{G} to be a glide reflection of **minimal** gliding vector in figure 8.5, we would be in trouble; for 'playing by the rules' led to a glide reflection \mathbf{G}_0 of gliding vector strictly smaller than that of \mathbf{G} -- to be precise, **one third** the length of \mathbf{G} 's gliding vector! And we have every right, in fact obligation, to **assume** the existence of a minimal gliding

vector: if that is not the case, then, **squaring** glide reflections of arbitrarily small gliding vectors would imply the existence of a pattern with arbitrarily small translations, violating Loeb's **Postulate of Closest Approach** (4.0.4).

Looking back at 8.1.3 and figure 8.6, it becomes clear that what 'created' \mathbf{G}_0 and its 'smaller than minimal' gliding vector was \mathbf{T}_2^{-1} , the component of \mathbf{T}^{-1} that is parallel to \mathbf{G} . At this point, you may ask: aren't we bound to always run into trouble, with \mathbf{T}_2^{-1} always creating a glide reflection having a gliding vector **shorter** than \mathbf{T}_0 ?

Perhaps the best way to answer this question is to have a closer look at figure 8.7 and its 'apparently legal' **pg** pattern: what happens when we compose its minimal glide reflection \mathbf{G}_0 with \mathbf{T} ? In simpler terms, what happens when \mathbf{T}_2^{-1} is added to \mathbf{G}_0 's minimal vector \mathbf{T}_0 ? Since $\mathbf{T}_2^{-1} = -2 \times \mathbf{T}_0$ (figure 8.7), the result is $\mathbf{T}_0 + \mathbf{T}_2^{-1} = \mathbf{T}_0 + (-2 \times \mathbf{T}_0) = -\mathbf{T}_0$, which is \mathbf{G}_0^{-1} 's gliding vector: we 'jumped' from \mathbf{T}_0 to $-\mathbf{T}_0$ (as opposed to a still downward vector shorter than \mathbf{T}_0) only because \mathbf{T}_2 wasn't any shorter -- because \mathbf{T}_2 itself is **minimal** as the **vertical component** of **any** valid translation of the **pg** pattern in figure 8.7!

[More generally, $\mathbf{T}_0 + m \times \mathbf{T}_2 = (2m+1) \times \mathbf{T}_0$ for **all** integers m : the resulting gliding vector is, according to our discussion in 8.1.3, still 'legal', corresponding to a **valid** glide reflection. Even more generally, notice that $\mathbf{T}_0 + \mathbf{t}$ is an **odd** ('legal') multiple of \mathbf{T}_0 if and only if the 'vertical' translation \mathbf{t} is an **even** multiple of \mathbf{T}_0 (hence an arbitrary multiple of \mathbf{T}_2). Conversely, the composition of two vertical glide reflections of the form $(\mathbf{M}, k_1 \times \mathbf{T}_0)$ and $(\mathbf{M}, k_2 \times \mathbf{T}_0)$, where k_1 and k_2 are **odd** integers, is a **translation**, with $k_1 + k_2$ **even**, of vertical component $(k_1 + k_2) \times \mathbf{T}_0$: we can therefore say that all valid translations have a parallel-to-axis component of the form $k \times \mathbf{T}_0$, where k is an **even** integer.]

Putting everything together, and with our remarks in 8.1.7 further below also in mind, we get a **condition of existence** for **pg**, the pattern first studied in sections 4.3 and 6.2:

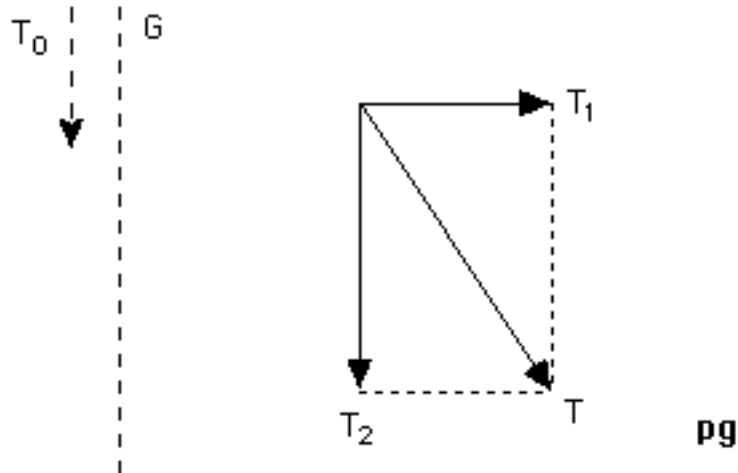


Fig. 8.8

In English: in a **pg** pattern, its translation's minimal parallel-to-the-gliding-axis component (T_2) must be the double of its glide reflection's minimal gliding vector (T_0).

8.1.5 Two gliding vectors? Unpleasant as that may sound, we are not completely through with our derivation of the **pg** pattern! Indeed, while we have fully justified and understood figure 8.7's infinitely many, parallel and 'equal' glide reflections, running at equal distances from each other, we never ruled out the existence of **another** glide reflection **half way** (Conjugacy Principle) between the axes of figure 8.7!

Luckily, that is not difficult to do: if t_1, t_2 are minimal gliding vectors for the glide reflection axes M_1, M_2 , respectively (and with M_1, M_2 parallel to each other by necessity), then their **squares** $2 \times t_1$ and $2 \times t_2$ are **translations** parallel to (M_1, t_1) and (M_2, t_2) ; so, by 7.4.1, $(M_1, t_1 - 2 \times t_2)$ and $(M_2, t_2 - 2 \times t_1)$ are **valid** glide reflections. The minimality assumptions on (M_1, t_1) and (M_2, t_2) lead then -- after switching from the two **collinear** vectors to their lengths -- to the inequalities $|t_1 - 2t_2| \geq t_1$ and $|t_2 - 2t_1| \geq t_2$, which **seem** to hold concurrently **if and only if** $t_1 = t_2$ (i.e., $t_1 = \pm t_2$, making the two glide reflections 'equal' to each other). Our argument is illustrated in figure 8.9, where $t_1 \neq t_2$ leads to a violation of the minimality

assumption about t_1 being the minimal vector for M_1 :

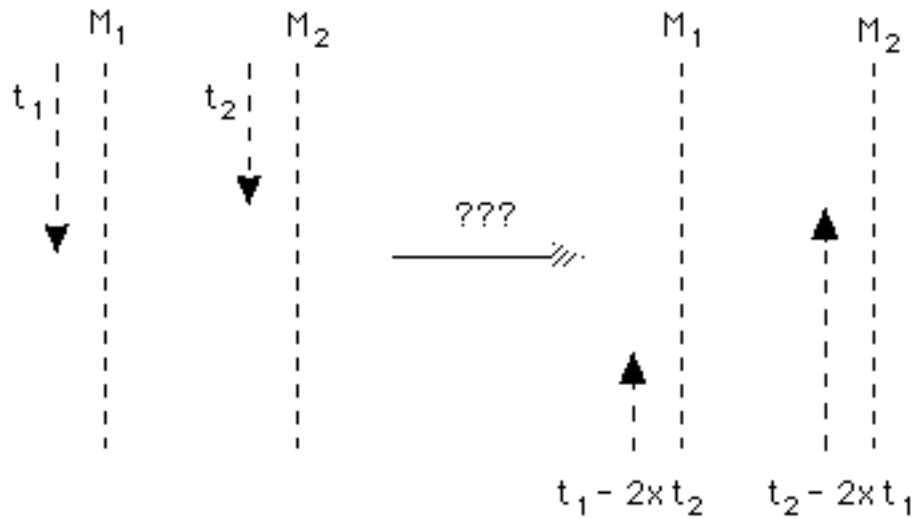


Fig. 8.9

Well, didn't we go a bit **too fast** with the algebra in the preceding paragraph? Let's see: squaring both inequalities we end up with $-4t_1t_2 + 4t_2^2 \geq 0$ and $-4t_1t_2 + 4t_1^2 \geq 0$, that is $t_2^2 \geq t_1t_2$ and $t_1^2 \geq t_1t_2$ or, equivalently, $t_2(t_2 - t_1) \geq 0$ and $t_1(t_1 - t_2) \geq 0$; now if $t_2 > 0$ and $t_1 > 0$, we may safely conclude $t_2 - t_1 \geq 0$ and $t_1 - t_2 \geq 0$, therefore $t_1 = t_2$ as above. Observe however that it is **possible** to have $t_2 = 0$ and $t_1 > 0$ **or** $t_1 = 0$ and $t_2 > 0$! (**Or** $t_1 = t_2 = 0$, of course.)

What is the geometric relevance of our algebraic observations? What corresponds to a glide reflection of minimal gliding vector of length **zero**? Luckily we are well prepared for this question, and the answer is: **reflection!** To be precise, a glide reflection employing a reflection axis, what we already know as a 'hidden glide reflection'.

8.1.6 A closer look at reflection. We have certainly seen as far back as in 1.4.8 that a reflection M may be viewed as a glide reflection of gliding vector zero. A natural question to ask would be the following: what is M 's **next shortest** gliding vector? This question makes a lot of sense in view of what we have already discussed in this section: if T is the minimal gliding vector of a

glide reflection \mathbf{G} , then the next shortest vector is $3\times\mathbf{T}$ (8.1.4).

Alternatively, we may look at \mathbf{T}_0 , the shortest **non-zero** gliding vector of a (glide) reflection. In the case of a genuine glide reflection and a **pg** pattern, we have seen in figure 8.8 and 8.1.4 that $\mathbf{T}_0 = \mathbf{T}_2/2$, where \mathbf{T}_2 is always the translation's **minimal** vertical component. When it comes to reflection, we observed in 6.3.4 (figure 6.23), while studying two-colored **pm** patterns, how the existence of a vertical reflection \mathbf{M} does indeed **guarantee** $2\times\mathbf{T}_2$ as a valid vertical translation. That means that $2\times\mathbf{T}_2$ **must** be a gliding vector for the hidden glide reflection associated with \mathbf{M} , albeit **not necessarily** the shortest non-zero one (\mathbf{T}_0). Indeed a review of our examples in chapters 4 and 6 would certainly show that $\mathbf{T}_0 = 2\times\mathbf{T}_2$ holds for **cm** patterns only; in **pm** patterns it gives way to $\mathbf{T}_0 = \mathbf{T}_2$!

Leaving the **cm** aside for now, we could derive the symmetry plan for the **pm** (almost a '**special case**' of **pg**, studied in sections 4.2 and 6.3), arguing as in 8.1.2 through 8.1.4; we prefer to simply record the **pm**'s 'condition of existence':

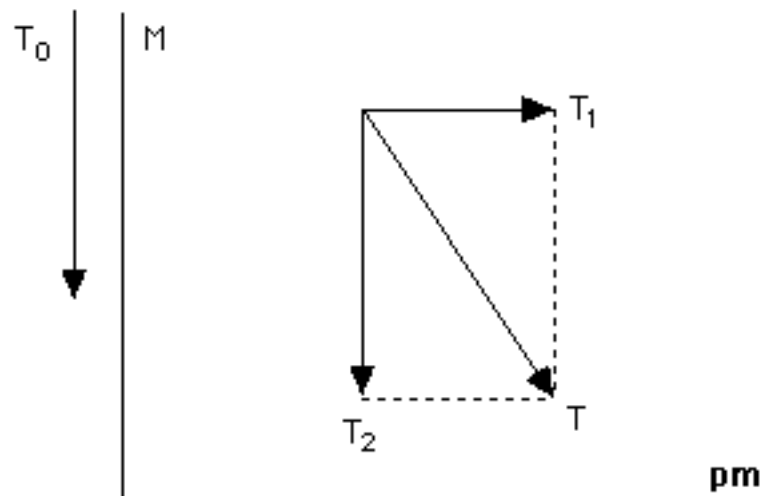


Fig. 8.10

In English: in a **pm** pattern, its translation's minimal parallel-to-the-gliding-axis component (\mathbf{T}_2) must be equal to the shortest non-zero gliding vector associated with its reflection (\mathbf{T}_0).

The next natural question: is $\mathbf{T}_0 = k \times \mathbf{T}_2$ possible for $1 < k < 2$ in the presence of reflection? (Notice that $k > 2$ is impossible by 6.3.4, while $k < 1$ would contradict the minimality of \mathbf{T}_2 at once: a gliding vector for a vertical reflection **must** in addition be a vertical translation vector -- **and** vice versa, of course, as noted above.) The answer is negative: with **both** $2 \times \mathbf{T}_2$ (6.3.4) and $k \times \mathbf{T}_2$ being vertical translations, their **difference** $(2-k) \times \mathbf{T}_2$ must **also** be a vertical translation, violating the minimality of $k \times \mathbf{T}_2 = \mathbf{T}_0$ via $0 < 2-k < k$. We illustrate our argument for $k = 5/4$ in figure 8.11 below:

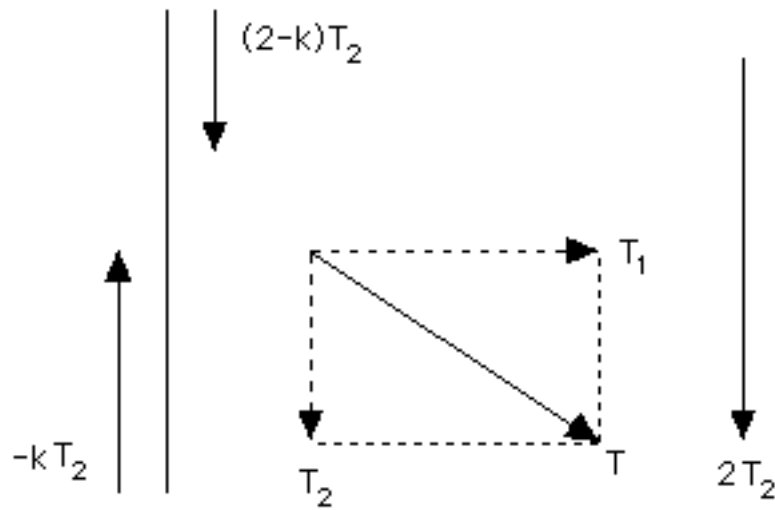


Fig. 8.11

8.1.7 Back to glide reflection. We have already seen in 8.1.4 and figure 8.8 that the **pg** pattern satisfies the relation $\mathbf{T}_0 = (1/2) \times \mathbf{T}_2$; at the same time, looking at the **cm** examples of chapters 4 and 6 we see that the vertical glide reflection's minimal gliding vector is **equal** to the translation's minimal vertical component: $\mathbf{T}_0 = \mathbf{T}_2$! Now we rule out all other possibilities (for a **glide** reflection **G**) in $\mathbf{T}_0 = k \times \mathbf{T}_2$, namely $k < 1/2$, $1/2 < k < 1$, $1 < k < 2$, and $k \geq 2$.

Ruling out $k < 1/2$ is the easiest of the four: indeed $2 \times \mathbf{T}_0 = 2k \times \mathbf{T}_2$ is a vertical translation, therefore minimality of \mathbf{T}_2 yields $2k \geq 1$.

We illustrate the case $1/2 < k < 1$ for $k = 3/4$ in figure 8.12:

assuming $T_0 = k \times T_2$ with $1/2 < k < 1$, we notice that $T'_2 = 2 \times T_0 - T_2 = (2k-1) \times T_2$ is **also** the vertical component of a **valid** translation, namely $T' = (-T) * (2 \times T_0) = (-T_1) * (-T_2) * (2k \times T_2) = (-T_1) * ((2k-1) \times T_2)$; but this contradicts the minimality of T_2 via $0 < 2k-1 < 1$.

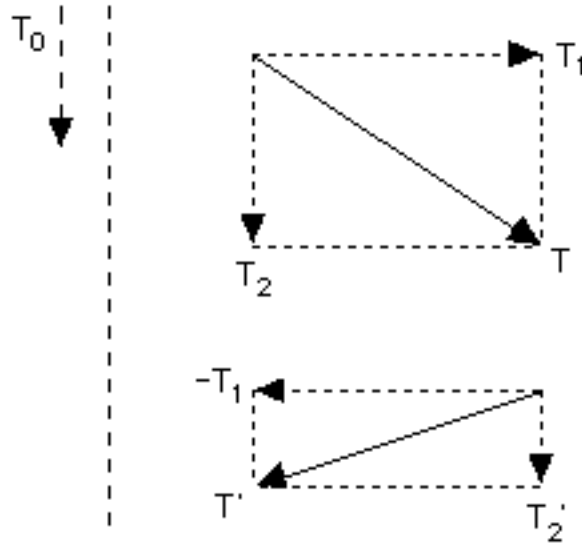


Fig. 8.12

As in the case of reflection (8.1.6, figure 8.11), the case $1 < k < 2$ is ruled out by appeal to the minimality of T_0 . Thanks to 7.4.1 the argument remains intact, except that 6.3.4 must be extended to glide reflection; in figure 8.13 we employ the Conjugacy Principle in order to show that $2 \times T_2 = T * (G[T])$ is **still** a valid vertical translation:

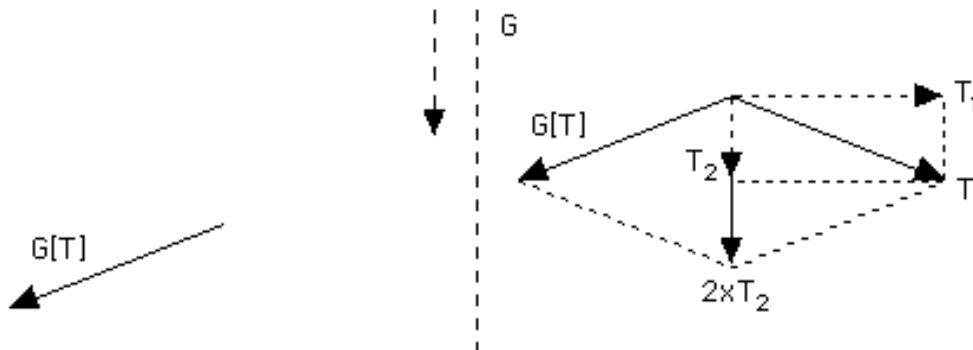


Fig. 8.13

Here is a **'direct'** approach to the matter (and in the spirit of

figure 6.23), corresponding to 8.1.6 and figure 8.11 (and $k = 5/4$), that you should ponder on your own:

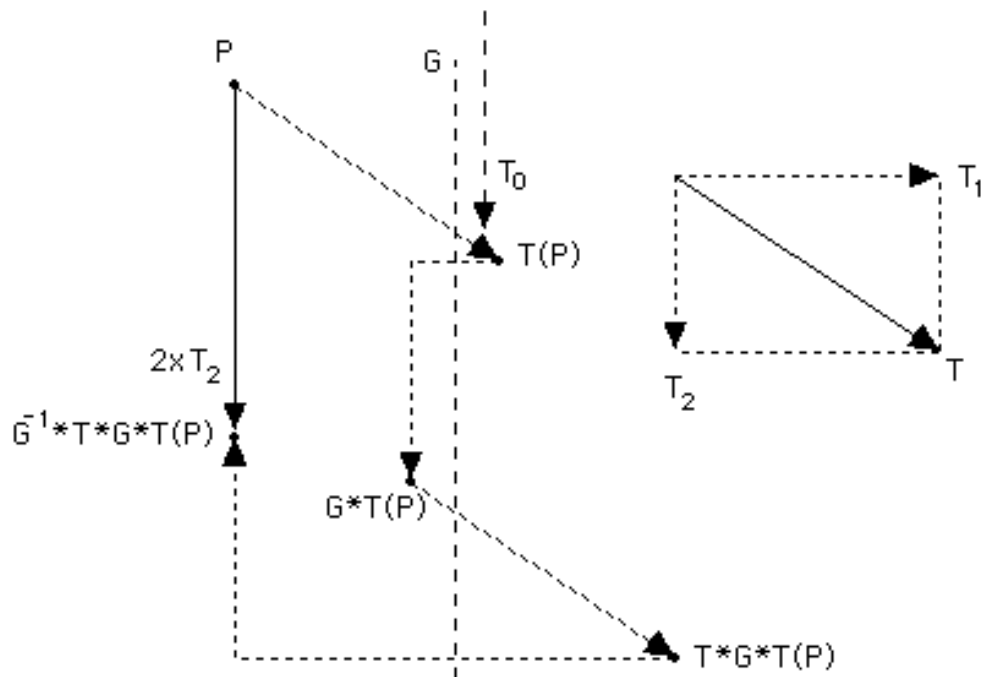


Fig. 8.14

Finally, we need to rule out the case $k \geq 2$. Since $2 \times T_2$ is a valid translation (figure 8.13), $T'_0 = T_0 - 2 \times T_2 = (k-2) \times T_2$ is **also** a gliding vector, corresponding (7.4.1) to the glide reflection $G * (-2 \times T_2)$; this contradicts the minimality of T_0 via $0 \leq k-2 < k$. (To be more precise, $k = 2$ yields a contradiction by turning the glide reflection into a **reflection**.)

So, while glide reflection is more 'complicated' than reflection, we have obtained a result **similar** to the one in 8.1.6: the glide reflection's minimal gliding vector T_0 is either **half** of or **equal** to the translation's minimal vertical component T_2 . (We stress again in passing a major difference between reflection and glide reflection: the former may employ **all multiples** of T_0 as gliding vectors, the latter only the **odd multiples** of T_0 .)

8.1.8 The last case. Summarizing, we point to a few useful facts already established:

-- two parallel glide reflections of distinct minimal gliding vectors may coexist if and only if one of them is a reflection (8.1.5)

-- the smallest non-zero gliding vector (\mathbf{T}_0) of a reflection \mathbf{M} may only be either equal or double the translation's minimal parallel-to- \mathbf{M} component (\mathbf{T}_2) (8.1.6)

-- the smallest gliding vector (\mathbf{T}_0) of a glide reflection \mathbf{G} may only be either equal or half the translation's minimal parallel-to- \mathbf{G} component (\mathbf{T}_2) (8.1.7)

In addition, we derived the **pg** (glide reflection only, $\mathbf{T}_0 = \mathbf{T}_2/2$) and **pm** (reflection only, $\mathbf{T}_0 = \mathbf{T}_2$) patterns (figures 8.8 & 8.10), corresponding to the equalities $t_1 = t_2 > 0$ and $t_1 = t_2 = 0$ of 8.1.5, respectively. Two natural questions would then be whether or not there exists a **reflection-only** pattern satisfying $\mathbf{T}_0 = 2 \times \mathbf{T}_2$ and whether or not there exists a **glide-reflection-only** pattern satisfying $\mathbf{T}_0 = \mathbf{T}_2$.

The first possibility is ruled out as follows:

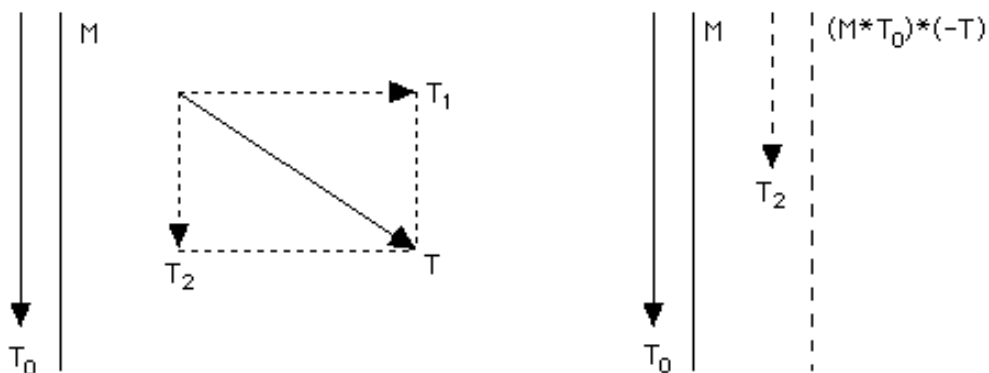


Fig. 8.15

Treating $\mathbf{M} * \mathbf{T}_0$ as a glide reflection and applying 7.4.1, we see that its composition with $\mathbf{T}^{-1} = -\mathbf{T}$ produces a **glide** reflection based on an axis at a distance of $|\mathbf{T}_1|/2$ to the right of \mathbf{M} and of gliding vector $\mathbf{T}_0 - \mathbf{T}_2 = \mathbf{T}_2$ (figure 8.15): this violates either \mathbf{T}_0 's

minimality (in case $(\mathbf{M} * \mathbf{T}_0) * \mathbf{T}^{-1}$ is indeed a reflection) or our assumption that **all** axes are **reflection** axes.

The second possibility is ruled out as follows:

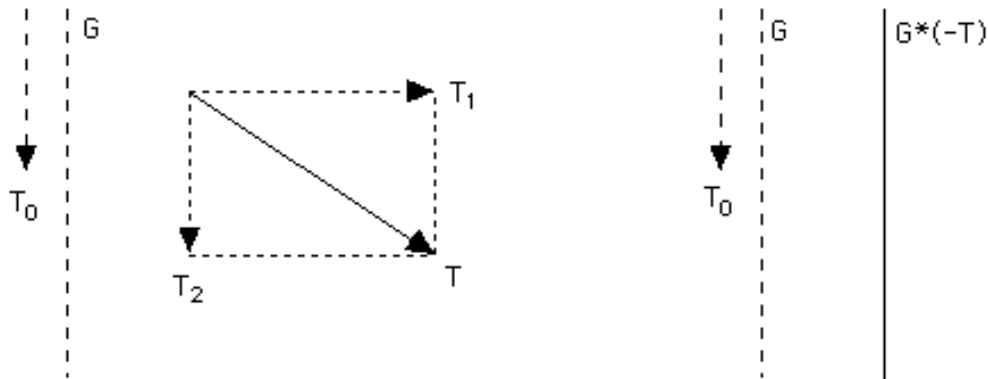


Fig. 8.16

Employing ideas from section 7.4 as in figure 8.15, we see that $\mathbf{G} * \mathbf{T}^{-1}$ is a **reflection** based on an axis at a distance of $|\mathbf{T}_1|/2$ to the right of \mathbf{G} (figure 8.16), again contradicting our starting assumption.

So, the only possibilities that remain are the ones corresponding to the case $t_1 > 0, t_2 = 0$ (or vice versa) of 8.1.5: reflection **and** glide reflection in one and the same pattern, at long last! Let \mathbf{T}_0^G be the minimal gliding vector of the glide reflection \mathbf{G} , and let \mathbf{T}_0^M be the minimal **non-zero** gliding vector associated with the reflection \mathbf{M} . With \mathbf{T}_2 being always the translation's minimal parallel-to- \mathbf{M} -and- \mathbf{G} component, there exist, in theory, four possibilities:

$$(I) \quad \mathbf{T}_0^G = \mathbf{T}_2/2, \quad \mathbf{T}_0^M = \mathbf{T}_2$$

$$(II) \quad \mathbf{T}_0^G = \mathbf{T}_2/2, \quad \mathbf{T}_0^M = 2 \times \mathbf{T}_2$$

$$(III) \quad \mathbf{T}_0^G = \mathbf{T}_2, \quad \mathbf{T}_0^M = \mathbf{T}_2$$

$$(IV) \quad \mathbf{T}_0^G = \mathbf{T}_2, \quad \mathbf{T}_0^M = 2 \times \mathbf{T}_2$$

It is easy to rule out (I) through (III). In (I) the composition of the reflection and the glide reflection yields a valid translation of 'vertical' component $\mathbf{T}_0^{\mathbf{G}} = \mathbf{T}_2/2$, contradicting \mathbf{T}_2 's minimality. In (II) the square of the glide reflection produces a valid translation \mathbf{T}_2 that contradicts the minimality of $\mathbf{T}_0^{\mathbf{M}} = 2 \times \mathbf{T}_2$. And in (III) the axis of \mathbf{G} ends up being a **reflection** axis for $\mathbf{G} * \mathbf{T}_2^{-1}$ -- recall that any gliding vector associated with a reflection axis is in fact a valid **translation** vector.

So the **only** remaining possibility is (IV), which is more or less already known to correspond to the only 360° pattern not 'formally' derived so far (good old **cm** of sections 4.4 and 6.4) and whose 'condition of existence' is given below:

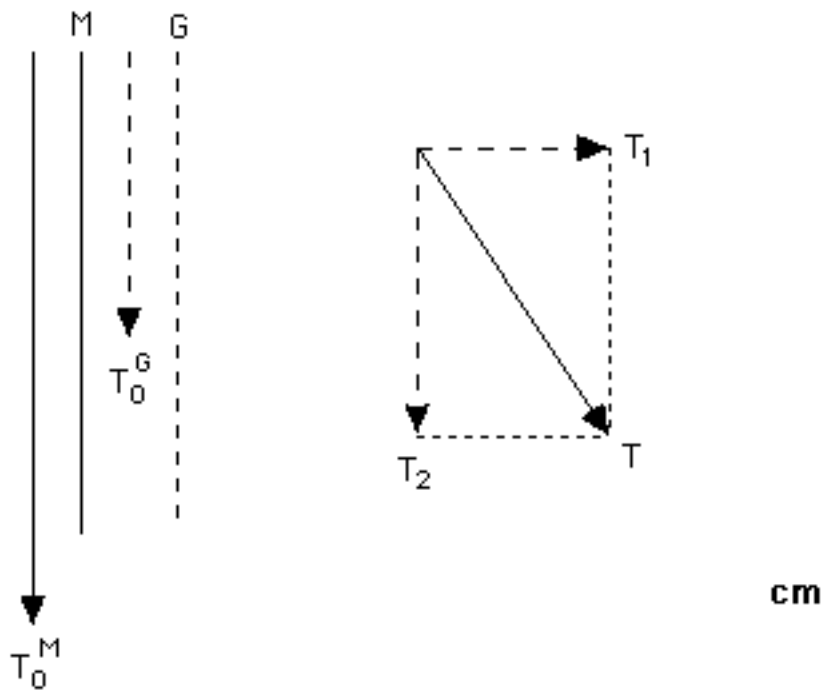


Fig. 8.17

Indeed we may verify figure 8.17 by reviewing old **cm** examples from chapters 4 and 6. No contradictions are to be found, glide reflection axes will never be good for reflection, whatever is supposed to be minimal will indeed remain minimal, etc. Of course $\mathbf{T} * \mathbf{M} = \mathbf{G}$, while \mathbf{T}_1 and \mathbf{T}_2 are **not** valid translations.

8.1.9 Brief overview. We have finally demonstrated why, in the presence of (glide) reflection and in the absence of rotation, only three types of wallpaper patterns are possible (**pg**, **pm**, **cm**); those are ‘**defined**’ in figures 8.8, 8.10, and 8.17, respectively, and are **characterized** by the relations $\mathbf{T}_0^G = \mathbf{T}_2/2$ (**pg**), $\mathbf{T}_0^M = \mathbf{T}_2$ (**pm**), and $\mathbf{T}_0^G = \mathbf{T}_2$ & $\mathbf{T}_0^M = 2 \times \mathbf{T}_2$ (**cm**). (The fact that these relations are indeed characterizations of the patterns in question follows from a closer look at our work in this section.) Together with the **p1** type (8.1.1), there exist therefore precisely **four** 360^0 wallpaper patterns.

In view of the characterizations and ‘definitions’ cited above for the three non-trivial 360^0 patterns, we need to **question** somewhat our discussion of the **cm** type in 6.4.5, where we viewed it as a ‘**merge**’ of **pg** and **pm**: **cm** has definitely its own structure, and it’s more than a **pg** and a **pm** ‘under the same roof’! Please have a look at the two-colored **cm** examples of figure 6.37 and notice how the removal of every other **row** yields a **pm** pattern, while the removal of every other **column** yields a **pg** pattern; in both cases the removal of half of the pattern **doubles** the vectors \mathbf{T} and \mathbf{T}_2 but leaves \mathbf{T}_0^G and \mathbf{T}_0^M unchanged, altering $\mathbf{T}_0^G = \mathbf{T}_2$ & $\mathbf{T}_0^M = 2 \times \mathbf{T}_2$ to $\mathbf{T}_0^M = \mathbf{T}_2$ (row removal, **pm**) or $\mathbf{T}_0^G = \mathbf{T}_2/2$ (column removal, **pg**).

One **important fact** to keep in mind: \mathbf{T}_2 (and hence $\mathbf{T}_1 = \mathbf{T} - \mathbf{T}_2$ as well) is a valid translation in both the **pg** and **pm** patterns, but **not** in the **cm** pattern; differently said, a translation’s projection onto the (glide) reflection direction (and its perpendicular) may **not** be a valid translation **if and only if** the 360^0 pattern is a **cm**.

The “if” part above is established through figure 8.17 and related comments. The “only if” follows from the observation that, in **any** pattern, the vertical component of **any** translation \mathbf{T}' must be an **integral** multiple of \mathbf{T}_2 ; but in both the **pm** and the **pg** the \mathbf{T}_2 is a valid translation, and so would be any integral multiple of it! (If the vertical component of \mathbf{T}' equals $k \times \mathbf{T}_2$ with k non-integer then the vertical component of the valid translation $\mathbf{T}' - m \times \mathbf{T}$, where m is the closest integer to k , would violate the minimality of \mathbf{T}_2 .)

8.2 180° patterns

8.2.1 The $p2$ lattice. In the absence of (glide) reflection, a 180° pattern is fully determined by an infinitude of half turn centers propagated by two non-parallel, '**shortest possible**' translations T_1, T_2 . This is demonstrated in figure 8.18, echoing figure 7.26 and related discussion in 7.6.4: please refer there for details.

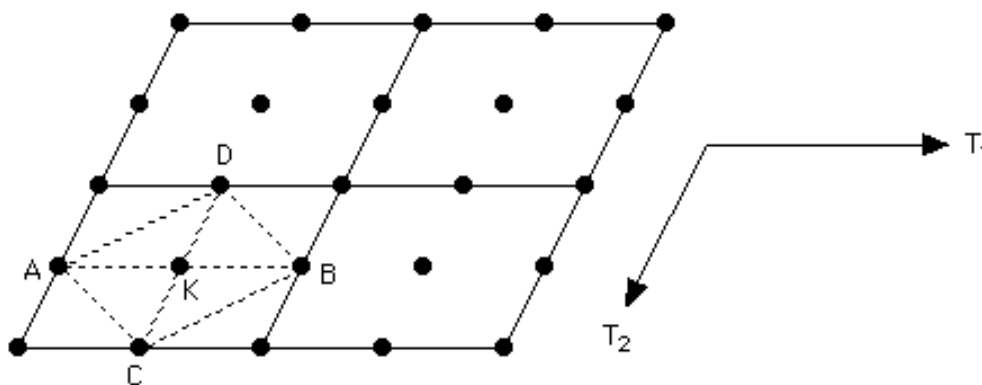


Fig. 8.18

The rows and columns of half turn centers of the $p2$ pattern in figure 8.18 would be **orthogonal** to each other in case there was some (glide) reflection (as in 8.2.3-8.2.6 below): indeed in such a case T_1 and T_2 would be **perpendicular** and **parallel**, respectively, to the (glide) reflection axis (as in figures 8.8, 8.10, and 8.17). Of course we do **not** need any (glide) reflection in order to make T_1 and T_2 perpendicular to each other and '**rule**' the 180° centers: see for example figures 4.28, 4.30, 6.39, and 6.40 in sections 4.5 and 6.5!

8.2.2 Ruling the centers. In the case you are not convinced by our argument above concerning the '**alignment**' of half turn centers by (glide) reflection, figure 8.19 offers another approach to the matter:

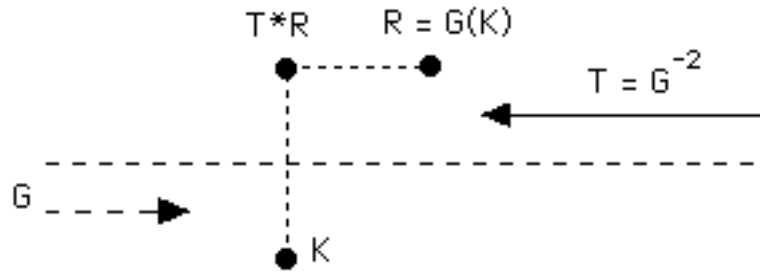


Fig. 8.19

Miraculously, \mathbf{G} not only glide-reflects K into a new center $\mathbf{G}(K)$ (Conjugacy Principle), but it also ends up **mirroring** it into another working center right across its axis: how did that happen? Well, as figure 8.19 suggests, the inverse of \mathbf{G} 's square is a '**backward**' translation \mathbf{T} ; composing \mathbf{T} with the half turn \mathbf{R} centered at $\mathbf{G}(K)$, and with \mathbf{T} going **second** (7.3.1, 7.6.4), creates a new rotation center **half way** between $\mathbf{G}(K)$ and $\mathbf{T}(\mathbf{G}(K))$, which is K 's mirror image!

Such observations are going to be crucial in what follows: assuming some (glide) reflection from here on, we will see how the 'ruled', orthogonalized lattice(s) of half turn centers are built, classifying 180° patterns at the same time. A solid departing point is to assume (glide) reflection in the pattern's 'vertical' direction: that **forces** (glide) reflection in the 'horizontal' direction as well, and in ways dictated by the laws that govern isometry composition; what is clear, in view of our results in section 8.1, is that there are precisely **three** possibilities for the vertical 'factor' (**pm**, **pg**, **cm**).

8.2.3 Starting with a **pm and an on-axis center.** We begin by assuming a **pm** vertical factor **and** the existence of one **180° center K on** one of the reflection axes. By the Conjugacy Principle, that center is translated all over that axis by multiples of \mathbf{T}_2 ; and then all the centers on that axis are translated across to **every other** reflection axis by multiples of \mathbf{T}_1 :

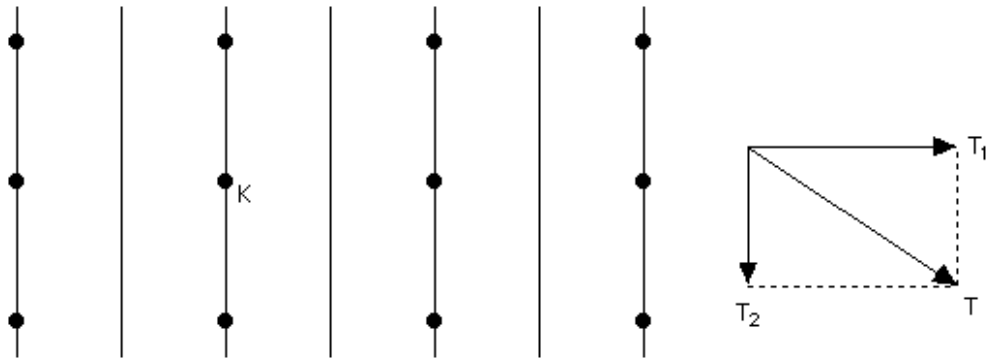


Fig. 8.20

Next come the compositions of the 'already existing' half turns with T_1 and T_2 , creating 'new' centers at distances of $|T_1|/2$, $|T_2|/2$ from the 'old' ones (7.6.4), inevitably lying on the reflection axes (which may be viewed as having been created by the same compositions):

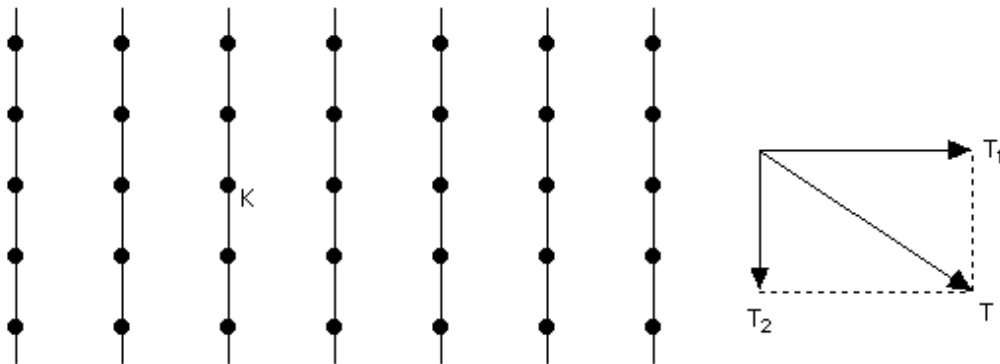


Fig. 8.21

Finally, the compositions of 180° rotations and reflections create 'new' reflection axes perpendicular to the existing ones and passing through the half turn centers (7.7.1):

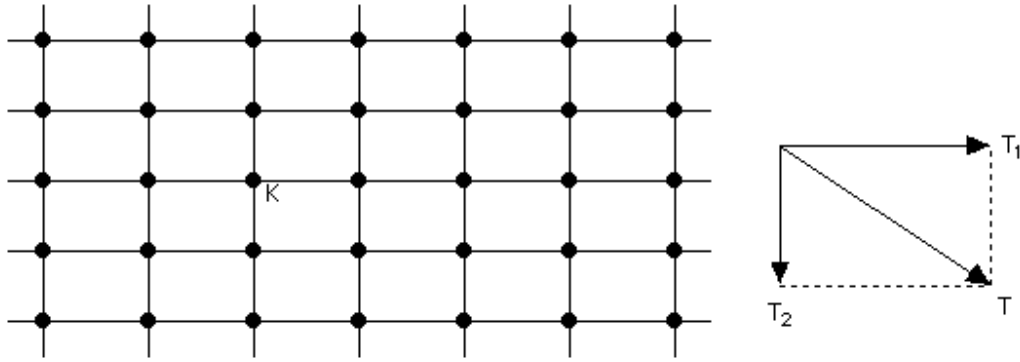


Fig. 8.22

What you see in figure 8.22 is the familiar **pmm = pm × pm** pattern of sections 4.6 and 6.8: no new isometry compositions are possible, everything is ‘**complete**’ and ‘**settled**’. Assuming minimality of **T₁** and **T₂**, **T** is the pattern’s **shortest** ‘diagonal’ translation; in particular, no translation (or any other isometry) may swap any two of the centers located at the corners of any given **smallest rectangle** in figure 8.22: this justifies our reference to ‘**four kinds**’ of half turn centers in 4.6.1.

8.2.4 Starting with a pm and an off-axis center. Let’s now assume a vertical **pm** factor and a 180° center **K** that does **not** lie on any of the vertical reflection axes. By the Conjugacy Principle, **K** must lie **half way** between two adjacent axes, **rotating** them onto each other; arguing then as in 8.2.3, we see that **K** is ‘multiplied’ by **T₁** and **T₂** into the group of centers shown in figure 8.23:

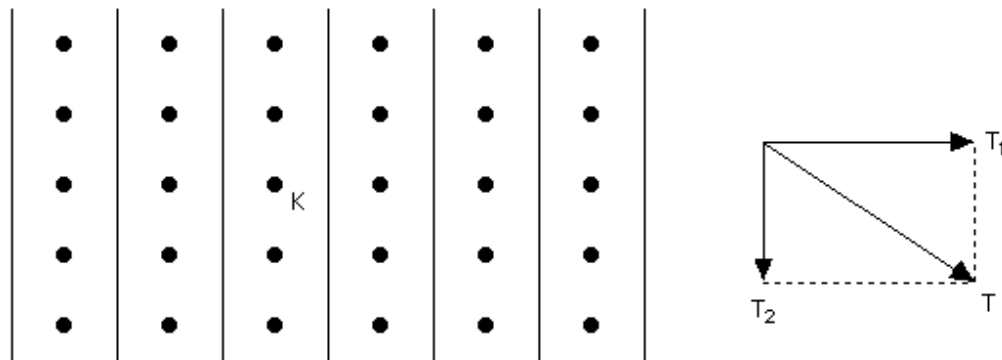


Fig. 8.23

Next, each composition of a 180° rotation and a reflection creates a glide reflection perpendicular to the reflection and passing through the rotation center (7.7.4), and of gliding vector of length $2x(|\mathbf{T}_1|/4) \times \sin(180^\circ/2) = |\mathbf{T}_1|/2$ (7.7.3). We end up with the 'complete' pattern of figure 8.24, which is the $\mathbf{pmg} = \mathbf{pm} \times \mathbf{pg}$ of sections 4.7 and 6.7:

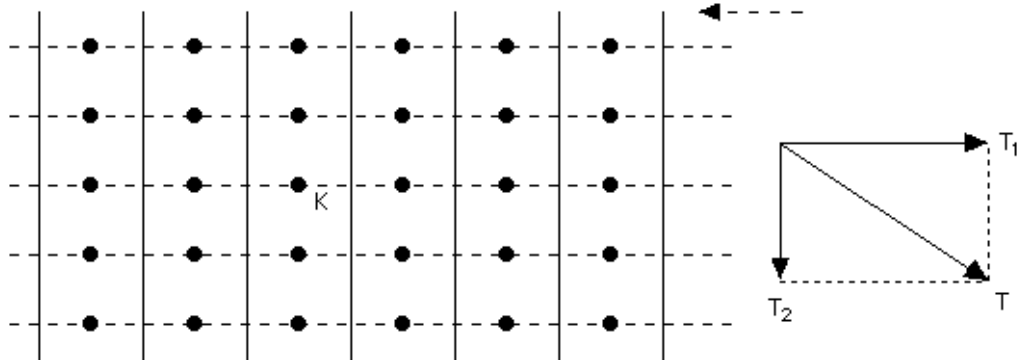


Fig. 8.24

Indeed the pattern's horizontal factor is a \mathbf{pg} , with its minimal gliding vector being half of \mathbf{T} 's horizontal component (8.1.4).

8.2.5 Starting with a \mathbf{pg} and an on-axis center. Let's now assume the existence of a \mathbf{pg} in the vertical direction **and** the existence of a 180° center K **on** a glide reflection axis. Exactly as in 8.2.3, the standard translations \mathbf{T}_1 and \mathbf{T}_2 'multiply' the half turn centers (still lying **on** the glide reflection axes); and, reversing the process of 8.2.4, each composition of a 180° rotation and a glide reflection of gliding vector $\mathbf{T}_2/2$ produces a reflection perpendicular to the glide reflection and at a distance of $(|\mathbf{T}_2/2|)/2 = |\mathbf{T}_2|/4$ from the rotation center (7.8.2). We end up with a horizontal \mathbf{pm} factor and, **again**, a \mathbf{pmg} pattern:

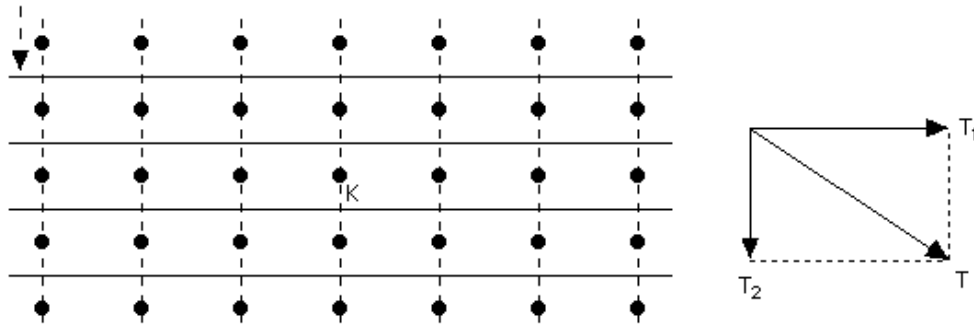


Fig. 8.25

Most certainly, the **pmg** patterns shown in figures 8.24 & 8.25 are mathematically indistinguishable. Looking at any '**smallest rectangle** of rotation centers' (as we did in 8.2.3), we see the four corners split into **two** pairs (4.11.2) of centers (lying on opposite sides) that may be swapped by **both** the pattern's reflection and the pattern's glide reflection.

8.2.6 Starting with a **pg and an off-axis center.** Assuming this time a vertical **pg** factor and a 180^0 rotation center **K** that does **not** lie on any glide reflection axis, we follow previous considerations in order to once more arrive at an 'aligned' **p2** lattice 'coexisting' with the **pg** pattern. As in 8.2.4, the Conjugacy Principle shows that **K**, and therefore all other centers created out of it via **T₁** and **T₂**, must lie half way between two adjacent glide reflection axes. Next, we appeal to 7.8.1 and 7.8.2 in order to see that each composition of a 180^0 rotation with a **vertical** glide reflection of gliding vector **T₂/2** lying at a distance $|\mathbf{T}_1|/4$ from its center creates a **horizontal** glide reflection of gliding vector of length $2 \times (|\mathbf{T}_1|/4) \times \sin(180^0/2) = |\mathbf{T}_1|/2$ at a distance of $(|\mathbf{T}_2/2|)/2 = |\mathbf{T}_2|/4$ from the rotation center (figure 8.26). The outcome is a horizontal **pg** factor and the familiar **pgg = pg × pg** pattern of sections 4.8 and 6.6.

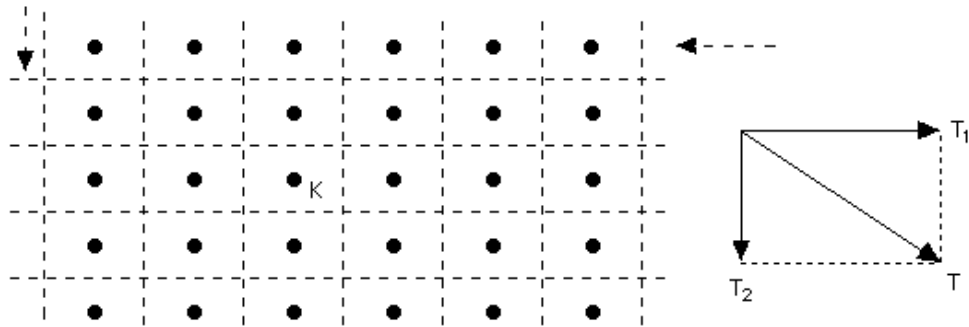


Fig. 8.26

Notice how the half turn centers in figure 8.26 are mirrored across glide reflection axes, precisely as shown in 8.2.2. Of course we did not directly appeal to glide reflection in order to get the **pgg** lattice; but notice that the **pgg**'s glide reflections allow 'travel' along the **diagonals** of that smallest rectangle of half turn centers: this confirms our remark about **two** kinds of **pgg** centers in 4.11.2!

8.2.7 Starting with a cm and a 'reflection' center. We have just verified in 8.2.3-8.2.6 that we may start with a **pm** vertical factor and end up with either a **pm** or **pg** horizontal factor, or that we may start with a **pg** vertical factor and end up with either a **pg** or **pm** horizontal factor. It seems that there is no way we can get a **cm** horizontal factor starting with either a **pm** or a **pg** in the vertical direction: for one thing, you may verify that there is **no way** we can insert a horizontal **in-between** (glide) reflection in figures 8.22 and 8.24-8.26 without creating, by way of isometry composition, **non-existing** (glide) reflection in the vertical direction.

In fact the coexistence of the **cm** with either the **pm** or the **pg** may be ruled out by our **crucial** remark at the end of 8.1.9: the **cm** **requires** a translation the vertical and horizontal components of which are not translations, which is **impossible** in either **pm** or **pg**!

So, let's **start** with a vertical **cm** and see what we get in the horizontal direction. (By symmetry between the two directions, we may **only** anticipate a horizontal **cm**; but we still have to verify that this **is** possible, after all, and also see in **how many** ways it is possible.) By the Conjugacy Principle, a 180^0 center K may only lie

on either a reflection or a glide reflection axis. Leaving the latter case for 8.2.8, we begin with K on a **reflection** axis, paralleling the 'center creation' process of 8.2.3 and figure 8.20:

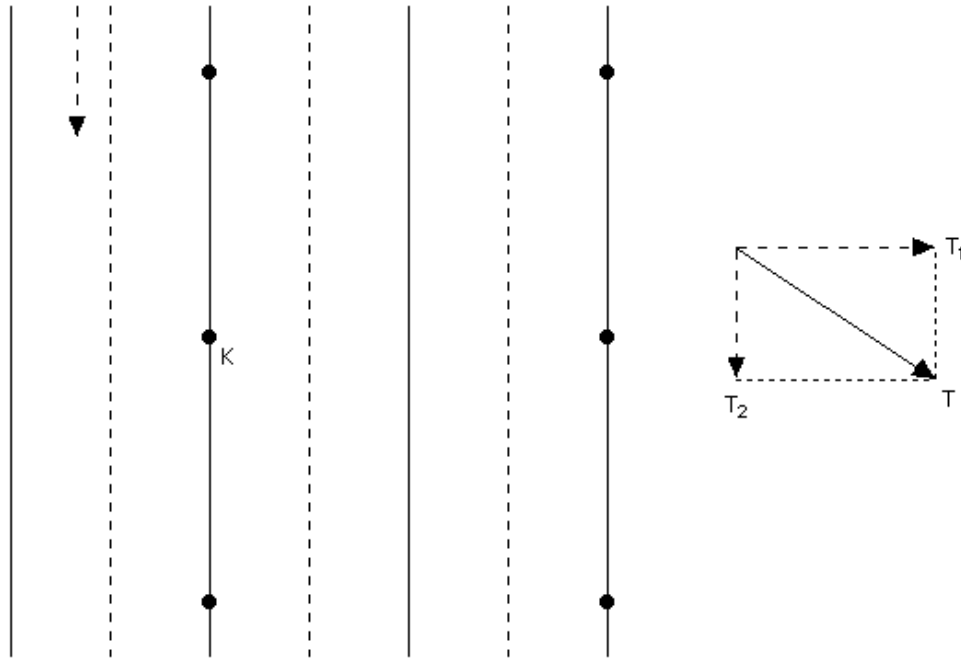


Fig. 8.27

The 180° centers featured in figure 8.27 are precisely those created out of K by way of **translation** and the Conjugacy Principle: recall at this point that the **cm's minimal** vertical and **minimal** horizontal translations are $2 \times T_2$ and $2 \times T_1$, respectively (8.1.8).

Next we **compose** the 'already existing' centers with the translations $2 \times T_2$ and $2 \times T_1$ (in the spirit of 7.6.4 and figure 8.21) in order to get 'new' centers, still on reflection axes **only** (figure 8.28); alternatively, we could get the same centers by employing the glide reflections and 8.2.2:

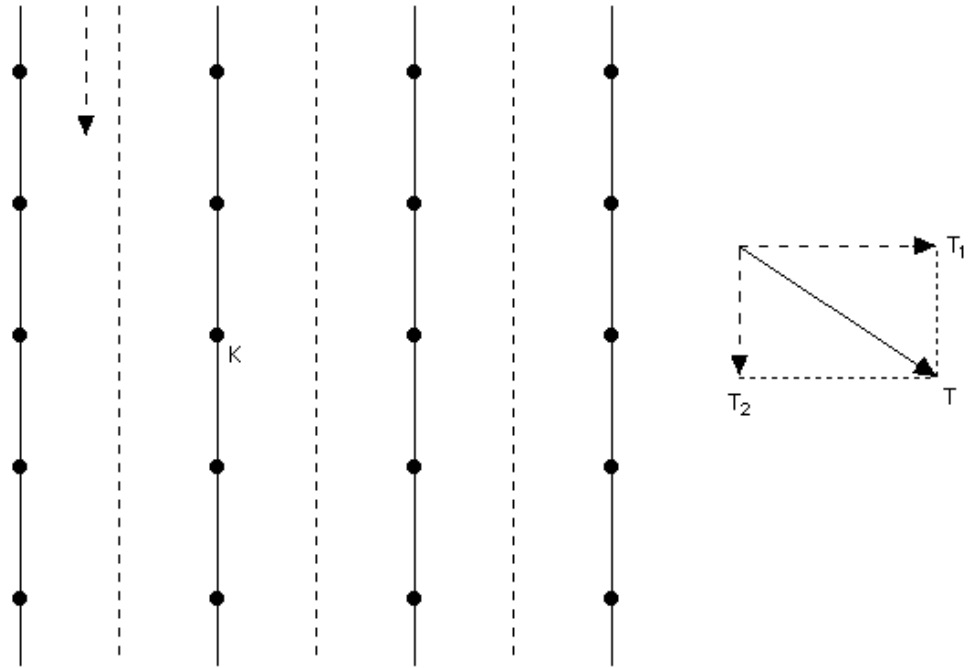


Fig. 8.28

Now the vertical reflections **'turn'** into horizontal reflections, exactly as in figure 8.22:

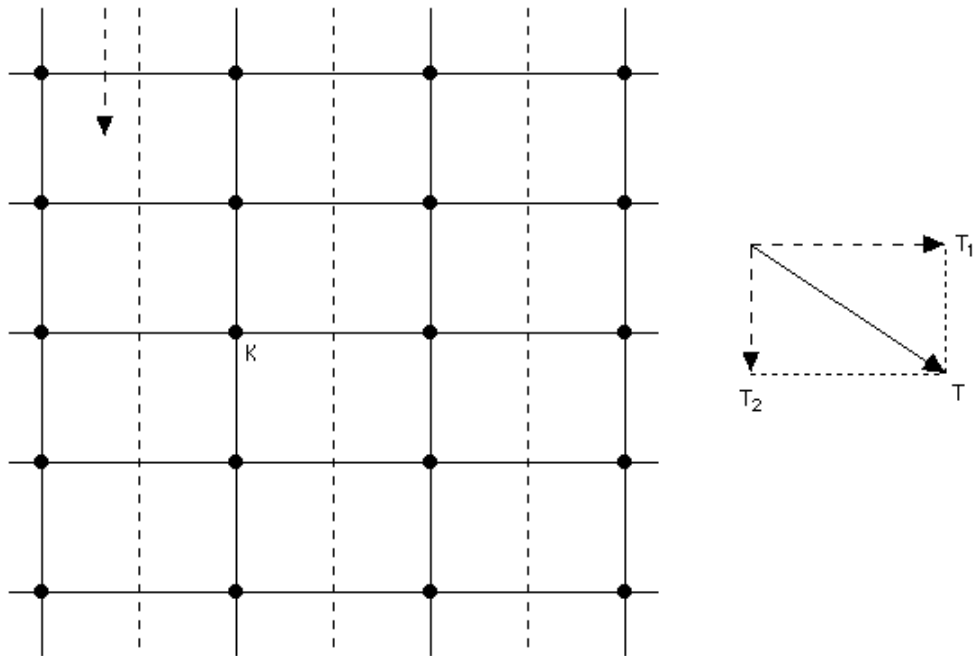


Fig. 8.29

Next come the horizontal glide reflections, 'created', as in 8.2.6 and figure 8.26, by compositions of vertical glide reflections with 180° rotations the centers of which do not lie on the glide reflection axes. To be more specific, the composition of every vertical glide reflection of gliding vector \mathbf{T}_2 with a half turn center at a distance of $|\mathbf{T}_1|/2$ from it (figure 8.29) produces a horizontal glide reflection of gliding vector of length $2 \times (|\mathbf{T}_1|/2) \times \sin(180^\circ/2) = |\mathbf{T}_1|$ at a distance of $|\mathbf{T}_2|/2$ from the rotation center (7.8.1):

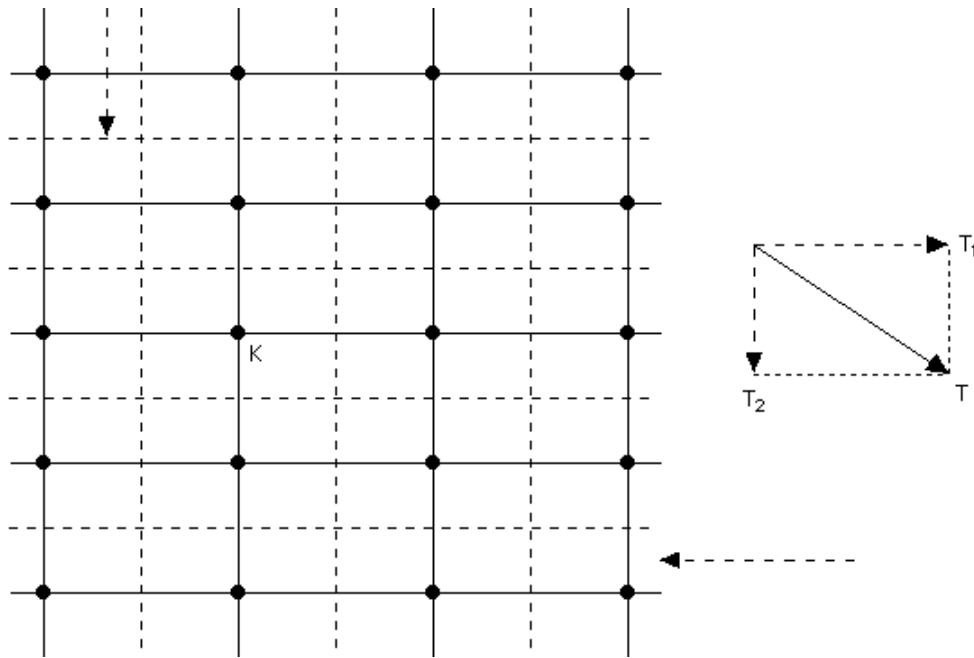


Fig. 8.30

Finally, every composition of a vertical glide reflection (of gliding vector \mathbf{T}_2) with a horizontal reflection produces a 180° center lying at the intersection of two glide reflection axes, and so does every composition of a vertical reflection with a horizontal glide reflection (of gliding vector \mathbf{T}_1). We demonstrate this in figure 8.31 below, relying either on section 7.9 or on figure 6.6.2: the shown half turn center and 180° rotation equals both $\mathbf{M}_1 * \mathbf{G}_2$ and $\mathbf{M}_2 * \mathbf{G}_1$, lying on \mathbf{G}_2 and at a distance $|\mathbf{T}_2|/2$ from its intersection with \mathbf{M}_1 , as well as on \mathbf{G}_1 and at a distance $|\mathbf{T}_1|/2$ from its intersection with \mathbf{M}_2 .

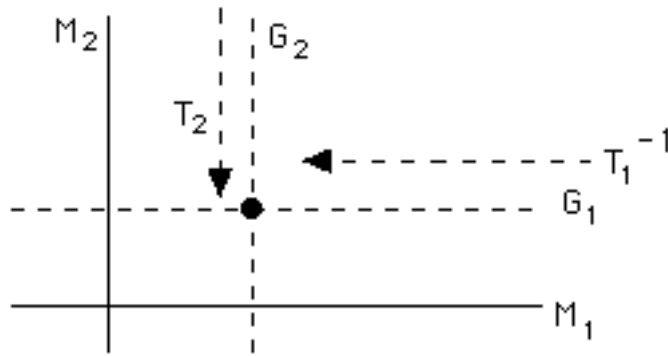


Fig. 8.31

Alternatively, we could at long last have used the **diagonal** translation \mathbf{T} and its **compositions** with 'existing' centers at the intersections of reflection axes (figure 8.30) to get the 'new' centers at the intersections of glide reflection axes. One way or another, we have finally arrived at the 'standard' $\mathbf{cmm} = \mathbf{cm} \times \mathbf{cm}$ pattern of sections 4.9 and 6.9, as no more centers or axes can be created:

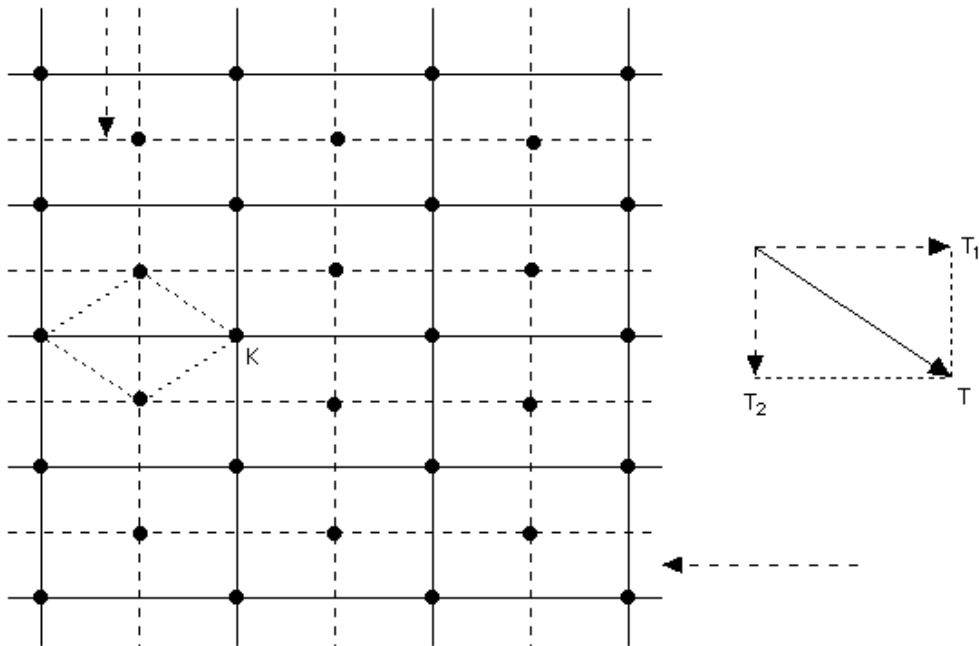


Fig. 8.32

Comparing the lattice of half centers in figure 8.32 (\mathbf{cmm}) to the ones in figures 8.22 (\mathbf{pmm}), 8.24 & 8.25 (\mathbf{pmg}), and 8.26 (\mathbf{pgg}), we can certainly say that this new lattice 'has been cut in half'; or,

if you prefer, while the minimal translation T remained the same, we moved from the 'minimal rectangle' of centers of the **pmm**, **pmg**, and **pgg** patterns to the **cmm**'s 'minimal rhombus' of centers, which is **twice** as large in area as that rectangle (figure 8.32).

8.2.8 Starting with a **cm** and a 'glide reflection' center. What happens in case the 'creating center' K lies on a vertical **glide** reflection axis? The answer may disappoint, but hopefully not astonish, you: we end up with exactly the **same cmm** pattern of figure 8.32, completing in fact the classification of 180° patterns! We leave it to you to check the details, providing just one **possible** 'intermediate stage' in figure 8.33: horizontal reflections have just been 'created' as compositions of vertical glide reflections and 180° rotations lying on them (as in 8.2.5); in the next stage, intersecting reflection axes will create all 'missing' half turn centers, etc.

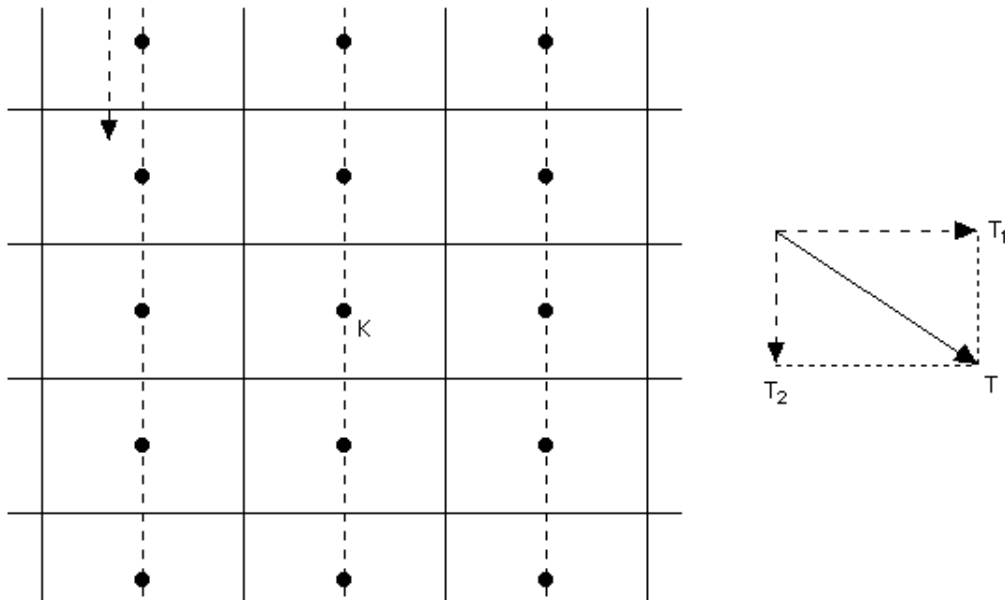


Fig. 8.33

Of course there was no way we were going to get anything but a **cm** in the horizontal direction (as already pointed out in 8.2.7). Still, we had to check that the horizontal **cm** factor would be the **same** in the two possible cases examined (half turn center on reflection axis or half turn center on glide reflection axis) in terms of translations, gliding vectors, etc; and figure 8.33 certainly makes that clear.

8.3 90° patterns

8.3.1 The lattice and the possibilities. It took us some time to 'build' the lattice of rotation centers for 180° patterns, be it with the help of translations only (**p2**, 7.6.4) or with the added assistance of (glide) reflection (**pgg**, **pmg**, **pmm**, **cmm** -- section 8.2). On the other hand, as we have seen in section 7.6, **just one** minimal translation suffices to build that lattice in the cases of 90°, 120°, and 60° patterns (starting from a **single** rotation center, always). This difference has dramatic consequences: unlike 180° lattices, all other lattices are **uniquely** determined and are **independent** of the (glide) reflection possibilities; in fact, as we will see below, it is now the lattice of rotation centers that **determines** the possible (glide) reflection interactions rather than the other way around!

To begin, observe that the lattice of rotation centers determines the **possible directions** of (glide) reflection in the case of a 90° pattern. Indeed the image of any segment AB, where A and B are two **closest possible** 90° centers, under **any** isometry could only run in **two** directions (figure 8.34); by 3.2.4, those yield at most **four** possible directions of (glide) reflection: images of AB under any two (glide) reflections are parallel if and only if their axes are either parallel or perpendicular to each other!

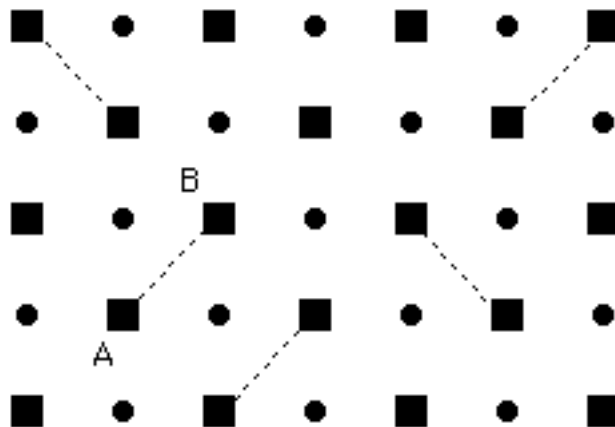


Fig. 8.34

Before we proceed into investigating the (glide) reflection structure of any given 90^0 pattern, we must of course ask: is there **any** (glide) reflection in the given pattern? If not, then the pattern only has 90^0 (and 180^0) rotation and translation, and it's no other than the familiar **p4** pattern of sections 4.12 and 6.10. Its structure has been discussed in 7.6.3 and it is also going to be further investigated in 8.3.2 below ... precisely because it is destined to play a very important role **even** in the presence of (glide) reflection!

8.3.2 Two fateful translations. Assuming from now on that our 90^0 pattern has (glide) reflection, let us notice first that sections 7.8 and 7.10 imply **precisely four** directions of (glide) reflection (indicated in fact in figures 8.34 and 8.35): **at least** four because the composition of a glide reflection with a 90^0 rotation generates another glide reflection making an angle of 45^0 with the original (section 7.8); and **at most** four because any two glide reflections intersecting each other at an angle smaller than 45^0 would generate a rotation by an angle smaller than 90^0 (section 7.10).

Further, the Conjugacy Principle implies that we must have the **same** type of **360^0 subpattern** in the 'vertical' and 'horizontal' directions (mapped to each other by the 90^0 rotation), and likewise for the two 'diagonal' directions; in particular, this **rules out** the **pmg** as a **180^0 subpattern**. Still, we are left, **in theory**, with **nine** combinations among **pmm**, **pgg**, and **cmm** 'factors'.

The way to eliminate most of these nine possibilities with very little work relies on the characterization of the **cm** pattern at the end of 8.1.9 **and** on the structure of the **p4** lattice investigated in 7.6.3 (and figure 7.23). Blending everything into figure 8.35 below, we examine whether or not the valid translations **t** and **T** may be analysed into valid translations in the diagonal and vertical-horizontal pair of directions, respectively:

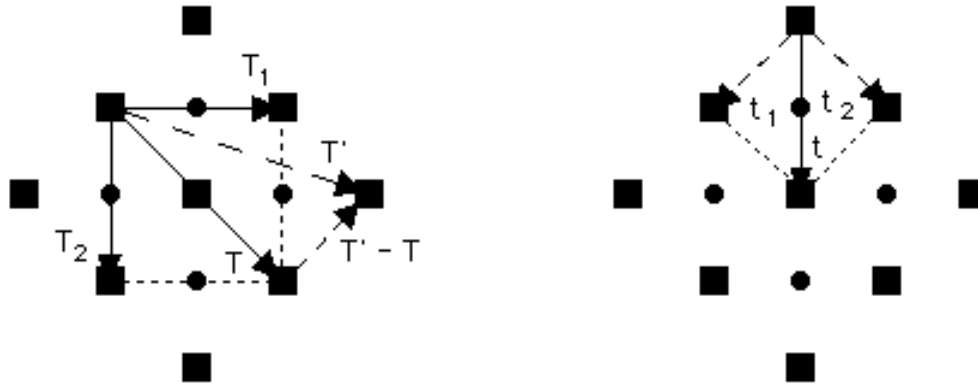


Fig. 8.35

On the right, the minimal vertical translation t may **certainly** be written as t_1+t_2 , where t_1 and t_2 are **not** valid **diagonal** translations. On the left, we see that valid translations such as T may be analysed into sums of two valid **vertical** and **horizontal** translations (like the **minimal** translations T_1 and T_2), while 'non-analyzable' translations such as T' are **not** valid to begin with (otherwise $T' - T$ would be a **valid** translation violating the minimality of T_1 or T_2); in fact some further analysis would easily show that **every** valid translation may only have **valid** vertical and horizontal components. (Here is a way to confirm that: observe that we may introduce a coordinate system so that all rotation centers have **integer** coordinates, the twofold centers one even and one odd, the fourfold centers either two even coordinates ('**even**' centers) or two odd coordinates ('**odd**' centers); a translation would then be valid if and only if it 'connects' two odd centers or, **equivalently**, two even centers -- that is if and only if it is of the form $\langle 2k, 2l \rangle = k \times T_1 - l \times T_2$, where $T_1 = \langle 2, 0 \rangle$ and $T_2 = \langle 0, -2 \rangle$.)

In view of our crucial remark in 8.1.9, two conclusions follow at once: **one**, in the pattern's vertical-horizontal directions we may only have a **pmm** (two perpendicular **pms**) or **pgg** (two perpendicular **pgs**) subpattern; **two**, in the pattern's diagonal directions we may only have a **cmm** subpattern (two perpendicular **cms**).

Focusing first on the diagonal (**cmm**) directions, we notice that the Conjugacy Principle allows for **two** possibilities: reflections passing either through the **fourfold** centers (figure 8.36, left) or

through the **twofold** centers (figure 8.36, right).

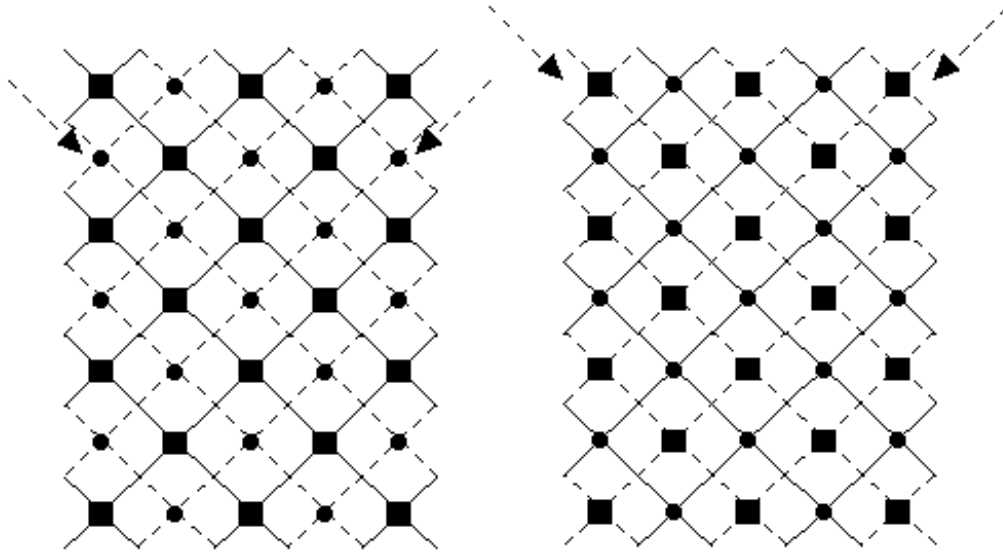


Fig. 8.36

Before examining the vertical-horizontal possibilities (**pmm** and **pgg**), let's have another look at the lattice of rotation centers in figure 8.36: while every two twofold centers may be mapped to each other by either a fourfold rotation (applied twice if necessary) or a translation, and every two fourfold centers on the right may be mapped to each other by some isometry (including a reflection or glide reflection), there exist fourfold centers on the left that may **not** be mapped to each other by any isometries; this is destined **not** to change (by the addition of vertical-horizontal isometries in figure 8.36), so the distinct notation for 'even' and 'odd' fourfold centers employed as early as in figure 4.5 is justified after all!

In theory, **each** of the two emerging 90° patterns of figure 8.36 should allow for **two** possibilities, **cmm** \times **pmm** and **cmm** \times **pgg**, bringing the maximum number of possible 90° patterns (with (glide) reflection) to **four**. But the actual situation is even simpler: by 7.7.1, we can only have either **none** or **four** reflections passing through a **fourfold** center; and this fact eliminates at once the **pgg** possibility on the left side and the **pmm** possibility on the right side of figure 8.36! So we are finally limited to **cmm** \times **pmm** on the left and **cmm** \times **pgg** on the right:

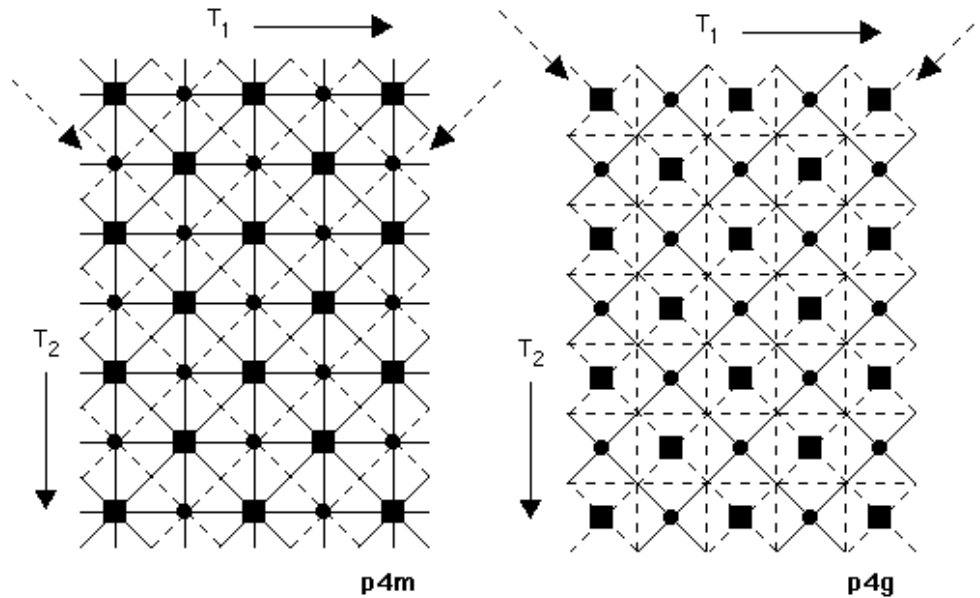


Fig. 8.37

But these patterns are the familiar **p4m** of sections 4.10 and 6.12 (left) and, after rotation by 45° , **p4g** of sections 4.11 and 6.11 (right): the classification of the 90° patterns is now complete.

8.4 120° and 60° patterns

8.4.1 Two families, one lattice. The reason we are studying 120° patterns and 60° patterns in the same section is that, to a large extent, these two types share the same lattice of rotation centers. Let's have a look at the two lattices in figure 7.24 (**p3**, smallest rotation 120°) and figure 7.25 (**p6**, smallest rotation 60°): if we ignore the 180° centers of the latter and view its 60° centers as 120° centers, then it would indeed be identical to the former!

8.4.2 Six possible directions. Let's now look at the **p3** lattice and the possibilities for (glide) reflection, observing that a valid (glide) reflection direction in the **p6** lattice **must** provide a valid (glide) reflection direction in the **p3** lattice, and, although not obvious, vice versa (8.4.4). We argue as in 8.3.1 and figure 8.34,

showing the underlying **hexagons** for clarity (figure 8.38); this time there are **three** possible directions for the image of AB, associated (via 3.2.4 again) with **six** possible directions of (glide) reflection:

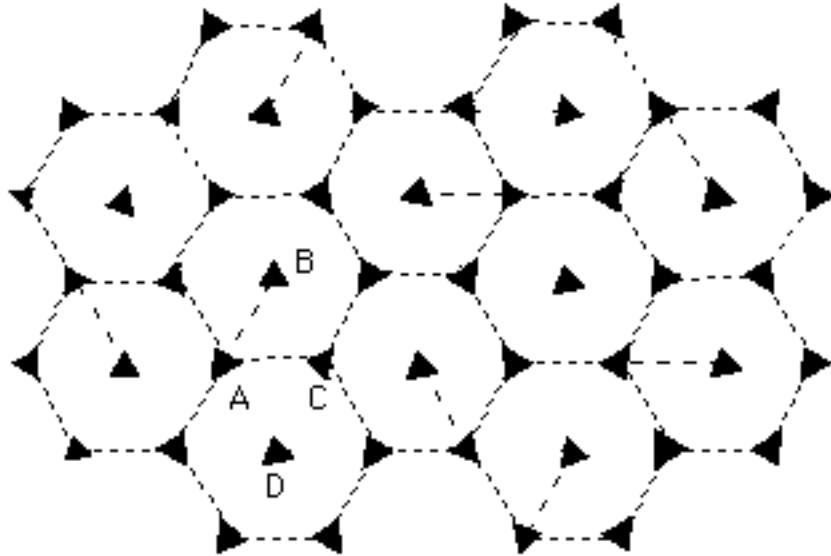


Fig. 8.38

Employing the methods of chapter 3 or otherwise, you should be able to see that the six possible directions are determined by pairs of either opposite vertices or opposite sides of any fixed hexagon (see figure 8.38). Assuming there is (glide) reflection, we need to decide, as we did in 8.3.2 for 90° patterns, **which type** among **pg**, **pm**, and **cm** we could get in each of the six directions; and, by the Conjugacy Principle (which **rotates** (glide) reflection axes by 120°), we actually need to check only **two** directions (one perpendicular to AB and one parallel to AB), and in just **one** stroke at that:

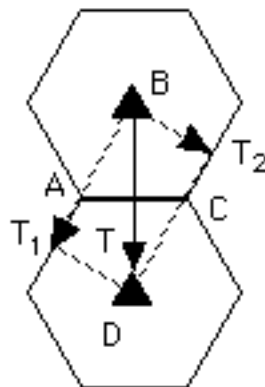


Fig. 8.39

What figure 8.39 offers is an analysis of the pattern's **minimal** (by 7.6.3) translation \mathbf{T} into two components **parallel** to the two glide reflection directions, **none** of which is a valid translation: by 8.1.9, we can only have a **cm** 'factor' in **each** of those directions!

8.4.3 Threefold types. In the absence of any (glide) reflection, a 120° pattern may only be the familiar **p3** pattern of sections 4.15 and 6.13, also investigated (in fact **derived**) in 7.6.3. If there is (glide) reflection, then it has to exist through a **cm** subpattern in precisely **three** of the six directions derived in 8.4.2. Specifically, and referring to figures 8.39 & 8.17, there exist two possibilities: **one**, a **cm** subpattern in the direction of \mathbf{T}_2 (plus that **rotated** by 120° both ways), with reflection axes at a distance of $|\mathbf{T}_1|$ from each other and in-between glide reflection of gliding vector \mathbf{T}_2 (figure 8.40, right); **two**, reversing the roles of \mathbf{T}_1 and \mathbf{T}_2 in figure 8.17, a **cm** subpattern in the direction of \mathbf{T}_1 (plus that rotated by 120° both ways), with reflection axes at a distance of $|\mathbf{T}_2|$ from each other and in-between glide reflection of gliding vector \mathbf{T}_1 (figure 8.40, left).

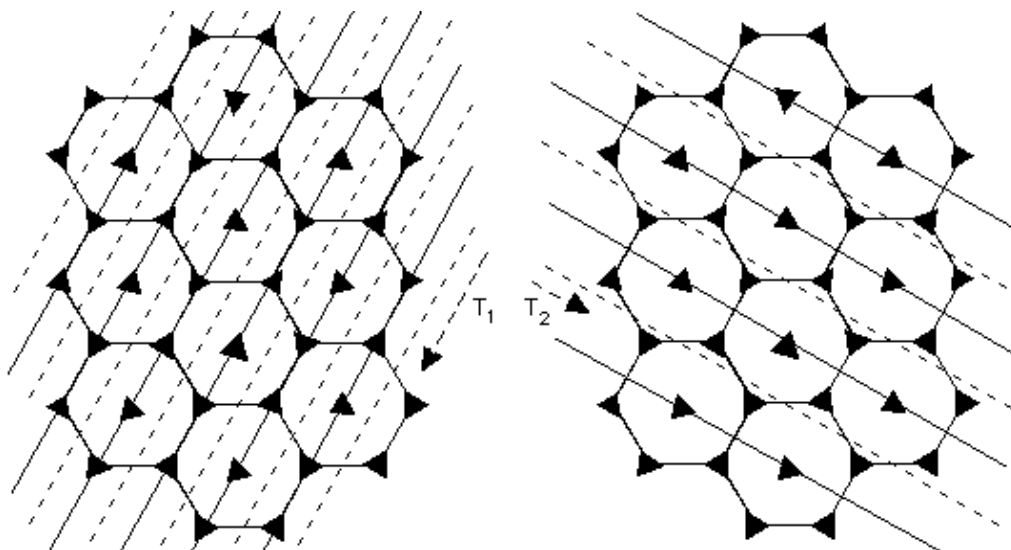


Fig. 8.40

A comparison between figure 8.36 (90° pattern generation) and figure 8.40 (120° pattern generation) is now appropriate: in figure

8.36, the direction of the two **cm** subpatterns was **uniquely** determined by the lattice, but there were **two** possible locations of the axes with respect to the centers; in figure 8.40, there are **two** possible **directions** of the three **cm** subpatterns, but the location of the axes with respect to the centers is **uniquely** determined within each of the two possible directions.

The **cm** subpatterns of figure 8.40 may now generate the two familiar 120° patterns shown in figure 8.41 (without the underlying hexagons or the gliding vectors): **p3m1** on the left (studied in sections 4.17 and 6.15) and **p31m** on the right (studied in sections 4.16 and 6.14); the classification of 120° patterns is now complete.

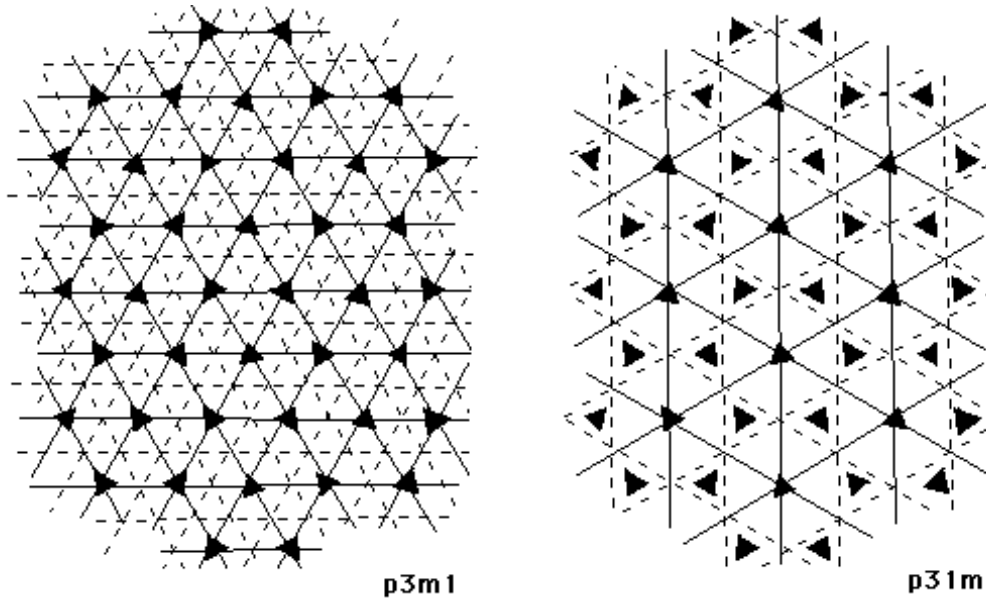


Fig. 8.41

Looking at figure 8.41 (or 8.40 for more clarity), we see that, remarkably, every two off-axis centers of the **p31m** may be mapped to each other by one of the pattern's isometries (notably (**glide reflection**)), while there exist indeed '**three kinds**' of centers in the **p3m1** (with no isometry swapping centers of different kind), and likewise in the **p3** (7.6.3): this confirms old observations from chapter 4! (Similar stories for 90° patterns: every two fourfold centers of a **p4g** are '**conjugate**' of each other (thanks to (glide reflection again), which is **not** true in either the **p4m** or the **p4**.)

8.4.4 Sixfold types. The last step of the classification is the easiest! Indeed, in the absence of any (glide) reflection there can only be the **p6** pattern of sections 4.14 and 6.16, also investigated (and **derived**) in 7.6.3. And in the presence of (glide) reflection, we need **all six** directions of 8.4.2, and it is still possible to show that we **must** have a **cm** subpattern in **all six** directions: all we need to do is make B and D **sixfold** centers in figure 8.39; and all other arguments and facts of 8.4.3 may also be extended, leading to the **p6m** pattern of sections 4.13 and 6.17 as the ‘**merge**’ of **p3m1** and **p31m** featured in figures 6.132 & 6.133 (and figure 8.41 as well)! Here it is in its full glory, with **T₁** and **T₂** playing the **same roles** as in 8.4.2 & 8.4.3 (and figure 8.40) -- and all ‘**old**’ glide reflections mapping **sixfold** centers to **sixfold** centers):

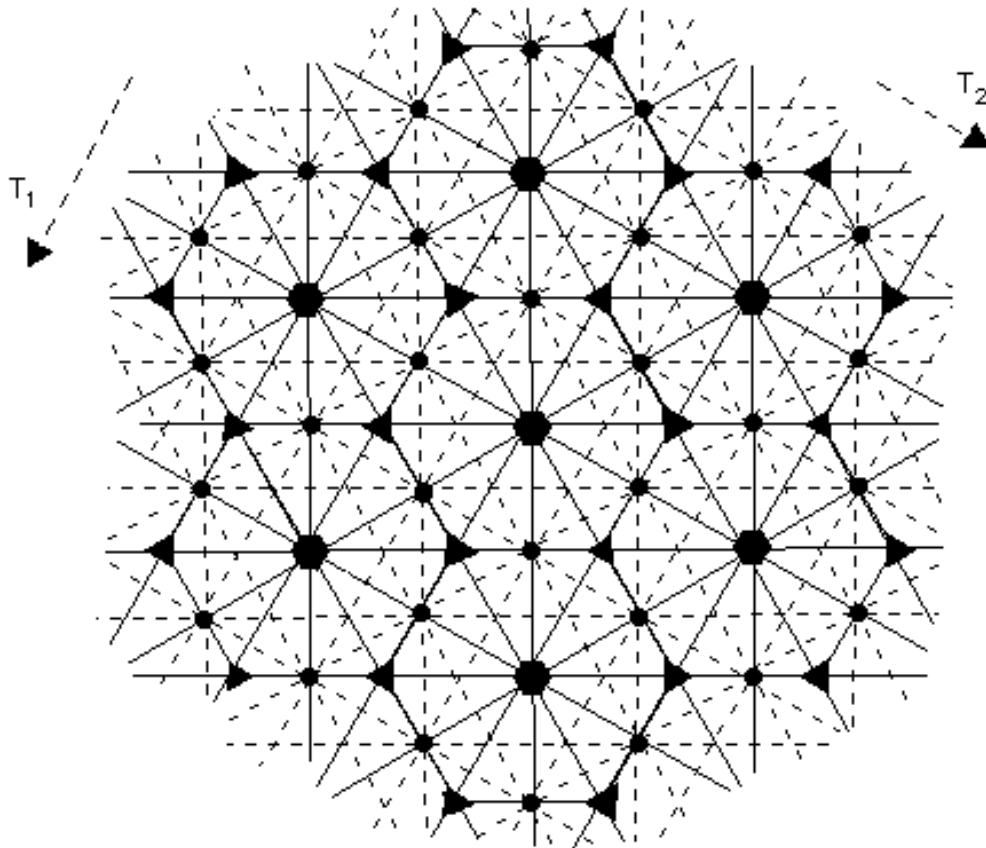


Fig. 8.42